Claremont Colleges
Scholarship @ Claremont

CGU Theses & Dissertations | CGU Student Scholarship

2019

Prediction of the Outcome in Cardiac Arrest Patients Undergoing Hypothermia Using EEG Wavelet Entropy

Hana Moshirvaziri
Claremont Graduate University

Follow this and additional works at: https://scholarship.claremont.edu/cgu_etd

Part of the Applied Mathematics Commons, Bioelectrical and Neuroengineering Commons, and the Neuroscience and Neurobiology Commons

Recommended Citation

Moshirvaziri, Hana. (2019). *Prediction of the Outcome in Cardiac Arrest Patients Undergoing Hypothermia Using EEG Wavelet Entropy*. CGU Theses & Dissertations, 514. https://scholarship.claremont.edu/cgu_etd/514.

This Open Access Dissertation is brought to you for free and open access by the CGU Student Scholarship at Scholarship @ Claremont. It has been accepted for inclusion in CGU Theses & Dissertations by an authorized administrator of Scholarship @ Claremont. For more information, please contact scholarship@cuc.claremont.edu.

PREDICTION OF THE OUTCOME IN CARDIAC ARREST PATIENTS UNDERGOING HYPOTHERMIA USING EEG WAVELET ENTROPY

By

Hana Moshirvaziri

Claremont Graduate University and California State University Long Beach

2019

APPROVAL OF THE DISSERTATION COMMITTEE

This dissertation has been duly read, reviewed, and critiqued by the Committee listed below, which hereby approves the manuscript of Hana Moshirvaziri as fulfilling the scope and quality requirements for meriting the degree of Ph.D.

Dr. Shadnaz Asgari, Chair

California State University, Long Beach

Biomedical Engineering Department, Chair

Dr. Ali Nadim, Co-chair

Claremont Graduate University

Institute of Mathematical Sciences (IMS), Professor

Dr. Marina Chugunova, Committee Member

Claremont Graduate University

Institute of Mathematical Sciences (IMS), Program Director

Dr. Perla Ayala, Committee Member

California State University, Long Beach

Biomedical Engineering Department, Assistant Professor

ABSTRACT

Prediction of the outcome in cardiac arrest patients undergoing hypothermia using EEG wavelet entropy

By: Hana Moshirvaziri

Claremont Graduate University: (2019)

Cardiac arrest (CA) is the leading cause of death in the United States. Induction of hypothermia has been found to improve the functional recovery of CA patients after resuscitation. However, there is no clear guideline for the clinicians yet to determine the prognosis of the CA when patients are treated with hypothermia. The present work aimed at the development of a prognostic marker for the CA patients undergoing hypothermia. A quantitative measure of the complexity of Electroencephalogram (EEG) signals, called wavelet sub-band entropy, was employed to predict the patients' outcomes. We hypothesized that the EEG signals of the patients who survived would demonstrate more complexity and consequently higher values of wavelet sub-band entropies.

A dataset of 16-channel EEG signals collected from CA patients undergoing hypothermia at Long Beach Memorial Medical Center was used to test the hypothesis. Following preprocessing of the signals and implementation of the wavelet transform, the wavelet sub-band entropies were calculated for different frequency bands and EEG channels. Then the values of wavelet sub-band entropies were compared among two groups of patients: survived vs. non-survived. Our results revealed that the brain high frequency oscillations (between 64-100 Hz) captured from the inferior frontal lobes are significantly more complex in the CA patients who survived (pvalue ≤ 0.02). Given that the non-invasive measurement of EEG is part of the standard clinical assessment for CA patients, the results of this study can enhance the management of the CA patients treated with hypothermia.

DEDICATION

To who that inspired it and will not read it…to my beloved grandmother, Mahboub.

ACKNOWLEDGMENT

I would like to gratefully acknowledge the guidance, support and encouragement of my doctoral advisor, Dr. Asgari, and the members of my committee during my time at University.

My gratitude extends to the Long Beach Memorial Hospital personnel and staffs specially Dr. Nima Ramezan the Medical Director of Neuroscience and Stroke Program at Long Beach Memorial Medical who have helped us in providing EEG data.

This research was partially supported by California State University, Long Beach College of Engineering Seed Grant, Memorial Medical Center Foundation Fund # 04600, and National Science Foundation Integrative Graduate Education and Research Traineeship Program (NSF IGERT) Grant #1069125.

TABLE OF CONTENTS

Chapter 1: statement of the problem 1

1.1 Background and statement of the problem 2

1.2 Research question and hypothesis, aim and objective 3

Chapter 2: Background information 4

2.1 Introduction 5

2.2 Brain waves Classification 5

2.3 EEG Applications 7

2.4 EEG signal acquisition techniques 9

2.4.1 Electrodes 10

2.4.2 Amplifier 11

2.4.3 Filters 11

2.4.4 Converter 12

2.4.5 Artefacts 12

2.5 EEG Signal Analysis 13

2.5.1 Signal enhancement and Feature extraction 13

2.6 Coma 14

2.7 Cardiac Arrest (CA) 14

2.8 Therapeutic hypothermia 15

2.9 Cardiac Arrest and Hypothermia: 16

Chapter 3: LITERATURE REVIEW [118] 17

3.1 *Introduction* 18

3.2 Materials and methods 18

3.3 Results 19

3.3.1 Conventional entropy‐based measures 25

3.3.2 Burst suppression measures 31

3.3.3 Information quantity measures 33

3.3.4 Combined measures 35

3.3.5 Enhanced cerebral recovery index 37

3.4 Discussion and conclusion 44

Chapter 4: STUDY DESIGN 49

4.1 Collection of the data 50

4.2 Patient's data 50

4.3 Patient demographic 51

4.4 Study Limitations 51

Chapter 5: DATA PROCESSING METHOD 52

5.1 Data processing steps 53

5.2 Preprocessing 53

5.3 Discrete Wavelet Transform 56

5.4 Wavelet Sub-band Entropy 57

5.5 ANOVA Mathematical Details 58

5.6 Statistical analysis 60

Chapter 6: SWE results 61

6.1 Results 62

6.2 Discussion and Conclusion 67

Chapter 7: Wavelet Coeficients SPECTRAL ENTROPY (WCSE) 69

7.1 Wavelet Coefficients Spectral Entropy (WCSE) 70

7.2 WCSE Method 71

7.3 WCSE Results 73

7.4 Discussion and Conclusion 76

7.5 Discussion on Left and Right Brain Hemisphere Differences 76

Chapter 8: SINGULAR-VALUE DECOMPOSITION (SVD) 79

8.1 Background: Question that was raised during the Qualification exam 80

8.2 Introduction to Singular-Value Decomposition (SVD) 80

8.3 K-mean clustering 81

8.4 SVD Analysis and K-mean clustering – Phase I 81

8.5 SVD Results- Phase I 82

8.6 More Analysis – Phase II 84

8.7 Results – Phase II 85

8.8 Conclusion 86

Appendix I 87

Appendix I – Phase I plots 88

Appendix II 91

Appendix II – Phase II plots 92

Chapter 9: REFERENCES 97

References 98

FIGURES

Figure 1: 1 second sample of EEG. 5

Figure 2: EEG waves. (a) Delta band ; (b) theta band (c) alpha band ; (d) beta band ; (e) gamma band Image reference [104] 7

Figure 3: Electrode locations of International 10-20 system for EEG (electroencephalography) recording (Picture form Wikipedia- public domain) 10

Figure 4: four lobes of the cerebral cortex (Picture source: Public Domain) 11

Figure 5: Therapeutic Hypothermia phases 15

Figure 6: A block diagram of the implemented EEG processing method 53

Figure 7: All EEG channels 54

Figure 8: Location of signals with high rate of noise to signal value 55

Figure 9: Daubechies3 wavelet function 56

Figure 10: filter tree algorithm for discrete wavelet transform (DWT) picture reference [105] 58

Figure 11: Check the normality of data for ANOVA (Sample plot) 62

Figure 12: Boxplots of high frequency oscillation sub-band (64-100 Hz) wavelet entropies over inferior frontal: A) F7 EEG channel; B) F8 EEG channel. 63

Figure 13: One-minute EEG signal captured from inferior frontal lobes (F7-F8) of A) a survived patient; B) a non-survived patient. 64

Figure 14: Location of F7 and F8 channels based on the 10-20 standard layout of EEG electrodes 65

Figure 15: Boxplots of high frequency oscillation sub-band (64-100 Hz) wavelet entropies over inferior frontal during Normo-thermia 65

Figure 16: Comparison between Hypothermia and Normothermia signals in Survived and Non-survived patients 66

Figure 17: Butterworth filters specification, A) Bandpass, B) Notch 72

Figure 18: Location of C3 and C5 channels based on the 10-20 standard layout of EEG electrodes 73

Figure 19: Boxplot of theta band frequencies (4-8 Hz) wavelet coefficients spectral entropies over C3 and F3 channels: A) F3 EEG channel, B) C3 EEG Channel 74

Figure 20: one minute EEG signal captured from C3 and F3 channels: A) Non-survived patient, B) Survived patient 75

Figure 21: EEG channels associated with good outcomes, Pink: WCSE results, Blue: SWE results 77

Figure 22: Sorted eigenvalues 82

Figure 23: Clustering results of survived and non-survived patients 83

Figure 24: clustering result for channels 1 data points 85

Figure 25: clustering result for channels 2 data points 86

TABLES

Table 1: List of selected publications along with a summary of their results (ordered based on the year of publication) 19

Table 2: Summary of the State-of-the-Art in employment of quantitative EEG measures (features) for prognostication of outcome in the cardiac arrest subjects treated with hypothermia 41

Table 3: Patient demographic 51

Table 4: summary of K-mean results 83

CHAPTER 1: STATEMENT OF THE PROBLEM

1.1 Background and statement of the problem

Cardiac arrest (CA) is the leading cause of death in the United States [1, 2]. Each year, about 325,000 people have an out-of-hospital cardiac arrest, whereas only 10–20% of them survive [3, 4]. Poor functional outcomes such as moderate to severe disability or persistent vegetative state are common among the survivors [5, 6]. Early and accurate prediction of CA outcome is of tremendous value both in terms of (a) optimizing the clinical treatment/intervention, and (b) health care cost management. The accurate prognosis of CA would also help families of the patients to make a better-informed decision with respect to potential life support withdrawal versus continued supportive care [7].

In addition to higher survival rate and better functional outcome, therapeutic hypothermia (TH) has been associated with shorter hospital stay duration for CA patients [8,9]. Thus, TH has recently become a standard of care after resuscitation [9]. However, CA outcome prognostication for the patients treated with TH is currently qualitative and poorly understood [7, 10]. This is mainly due to the use of sedative and paralytic agents, and neuroprotective effects of hypothermia that reduce sensitivity of the conventional CA prognostication markers and/or change their optimal timing for the outcome prediction [7, 9, 11–15].

Recent studies have shown that electroencephalography (EEG) can be useful in CA outcome prediction [9]. For example, several EEG patterns (including the absence of EEG reactivity, the presence of burst suppression with generalized epileptiform activity, and the presence of generalized periodic complexes on a flat background) have been associated with poor outcome [16, 17]. In contrast to other prognostication modalities, EEG measurement can be performed easily, continuously and noninvasively at the patient's bedside. But visual EEG pattern recognition is laborious and subjective [18]. It also requires a specialized training in EEG interpretation and

many nurses and physicians in intensive care units (ICUs) lack such expertise [19]. Recent advances in the quantitative EEG analysis can overcome the above limitations [7, 20, 21]. As a result, over the last few years, there have been a growing interest in the development and employment of quantitative measures of EEG to predict CA outcome [22–28].

1.2 Research question and hypothesis, aim and objective

The present work aimed at the development of a prognostic marker for the CA patients undergoing hypothermia. A quantitative measure of the complexity of Electroencephalogram (EEG) signals, called wavelet sub-band entropy, was employed to predict the patients' outcomes. We hypothesized that the EEG signals of the patients who survived would demonstrate more complexity and consequently higher values of wavelet sub-band entropies.

The main goal of the study was to investigate whether this quantitative measure of EEG calculated over several frequency bands and EEG channels is significantly different between the subjects who survived and those who did not. The results of this investigation could potentially enhance the management of CA patients treated with hypothermia.

CHAPTER 2: BACKGROUND INFORMATION

2.1 Introduction

In 1875 English physician Richard Caton discovered that brain has electrical activities. The recorded EEG was demonstrated by Berger in the 1920s [90].

The activity of the brain neurons produces electrical and magnetic fields. These fields are recordable by means of electrodes. Depending on the distances of the recording electrode from the source of electrical activities we can record different signals from the brain. For example the local EEG is recorded from a short distance from the sources of brain electrical activities, however the EEG, in the most common sense is recorded from a longer distances, even from the scalp [90] EEG recording is known as an easy to use non-invasive acquisition method of brain signals with safety and high temporal resolution which can be applied repeatedly to patients. [93]

2.2 Brain waves Classification

EEG Signal is a non-stationary signal which has low spatial resolution [93] EEG signal is normally range from 0.5 to 100 µV in amplitude and a frequency in the range of about 1 Hz to 100 Hz [95] that is commonly sinusoidal which make it easy to measure it from peak to peak.

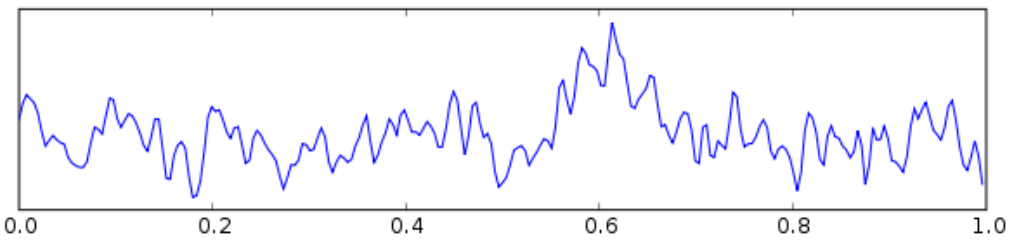

Figure 1: 1 second sample of EEG.

Image description (from Wikipedia): The signal was acquired in the Oz position processed with scipy and exported with matplolib. The momntage was with common derivation related to linked ears. The sampling rate was 256 Hz. Created by Hugo Gamboa Dez 2005

There are five patterns of brain wave shapes with certain range of frequencies exists: Gamma wave (>32), Beta wave (>16-32Hz), Alpha wave (8-16 Hz), Theta wave (4-8 Hz) and Delta wave (0.5 – 4 Hz) [92]. The precise frequency ranges associated with these waves are slightly different across studies [102].

Alpha rhythm is clearly is an oscillatory components of the human EEG [94] and with typical amplitude about 50 μV peak-peak can be usually observed better in the posterior and occipital regions of the brain. Closing the eyes, drowsiness and relaxation may induce the alpha waves, whereas any type of attention or alertness such as thinking, calculation and opening the eyes are put an end to this wave [91], [92]. It was suggested in several experiments that the speed of cognitive and good memory performance are indicated by about 1 hertz higher alpha frequencies [94].

Beta rhythms are dominates during normal state of wakefulness with open eyes [92] and have been recorded in olfactory brain area [90].

Theta is the dominant rhythm in the hippocampus area and can be captured during deep sleeping. Detecting the Changes in theta frequency are very difficult without the helping of sophisticated method. Alpha and theta respond in different and opposite ways. The crucial finding is that with increasing task demands theta synchronized, whereas alpha desynchronizes. That theta frequency varies as a function of alpha frequency and it was suggested to use alpha frequency as a common reference point for adjusting different frequency bands not only for the alpha, but theta range as well [94].

Delta rhythm are primarily associated with deep sleep and may be present in the waking state. It is very easy to confuse artefact signals caused by the large muscles of the neck and jaw with the genuine delta response [96].

Gamma wave is a signature of cognitive state and network dysfunction. Gamma power increases with cognitive phenomena such as perceptual grouping, attention, working memory and learning [102].

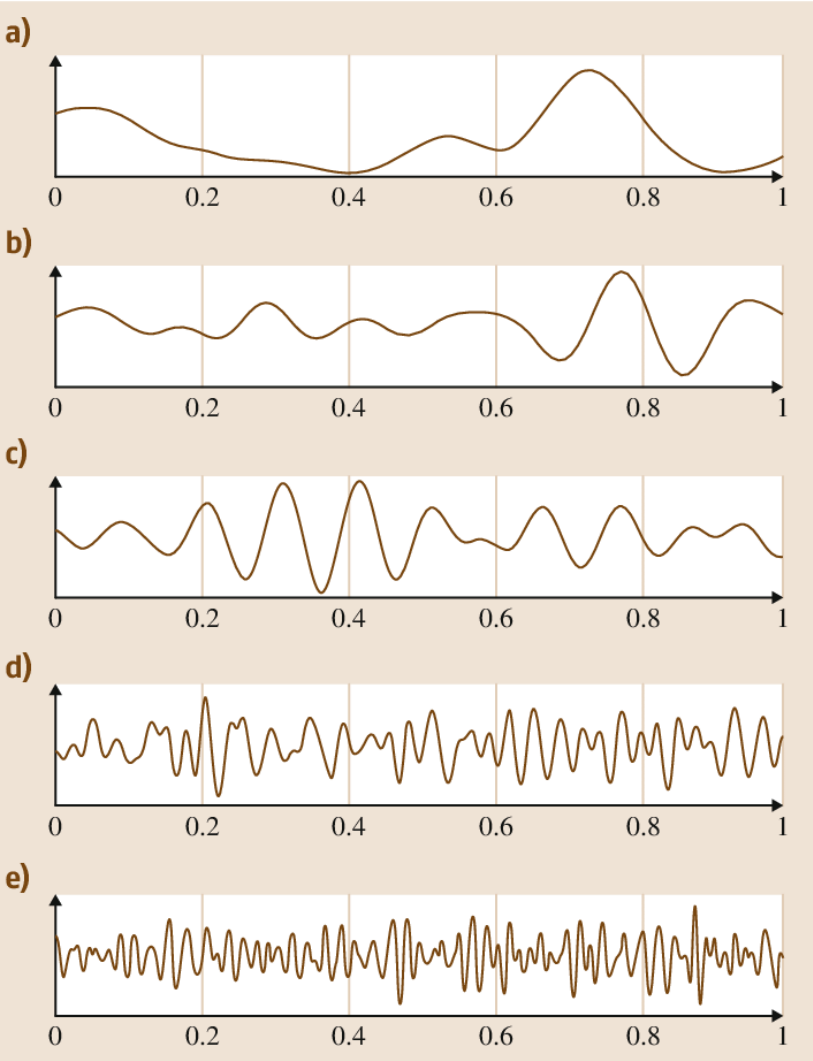

Figure 2: EEG waves. (a) Delta band ; (b) theta band (c) alpha band ; (d) beta band ; (e) gamma band Image reference [104]

2.3 EEG Applications

Neural activities' complex patterns after a stimulation can be recorded within a fractions of second by EEG. Therefore, although EEG signal provides less spatial resolution compared to MRI and

PED imaging methods, has the speed advantages. EEG often combined with MRI scan to get better information of strength and position of electrical activities in different parts of brain [92]

A few research and clinical applications of the EEG in humans and animals are listed below: [92]

- Monitor alertness, coma and brain death and cognitive engagement;
- Locate areas of Brain damage and test nerves pathways
- Control anesthesia depth
- Investigate epilepsy and locate seizure origin;
- Test epilepsy drug effects;
- Monitor human and animal brain development;
- Investigate sleep disorder and physiology.

Different brain activities have different EEG traces. Signal processing methods can help to distinguish the normal and abnormal brain activities [95]. Reduction in EEG signal amplitude, decrease of dominate frequencies beyond the normal limits of brain waves and production of spikes or special patterns are some example of some abnormality existence in the brain [92].

One of the useful application of EEG recording is the event related potential (ERP) or Evoked potential technique to study the brain cognitive processes. EPRs are significant voltage fluctuation resulting from evoked neural activity which is initiated by external or internal stimulus. During a mental task, the active region of the brain can be localized by PET and MRI and the time course of these activities defines by ERPs [92].

Quantitative EEG (QEEG) is another technique that by applying multichannel measurements can increase the ability of EEG to read data from the entire head simultaneously [93].

Another application of EEG is in Brain Computer Interface (BCI) which is a communication system. BCI is a process that makes use of the brain's output path way for conveying the commands and messages to the external world [93].

EEG Biofeedback or neuro-feedback uses the EEG signal for feedback input in a learning procedure for a subject to modify the brain activities. Biofeedback can help patient to normalize their behavior, stabilized mood and improve their mental performance [92].

2.4 EEG signal acquisition techniques

EEG recording system is consisted of four important elements:

Electrodes with conductive media which read the signal from the scalp, amplifiers with filters that amplified the microvolt signals in to the acceptable range to be digitalized accurately and filters to remove artefacts from the signal, Analog to digital converter to convert brain signal from analog to digital and finally recording device such as computers to store and display obtained data [93].

In mono channel EEG recording technique, the neural activity potential changes over the time are measured by a basic electric circuits which is consist of an active electrode and a reference electrodes. Also there is a ground electrode that calculates the differential voltages by subtracting the active electrode voltages and reference point. By increasing the number of active electrodes to 128 or 256 we can get the multi-channel configuration for EEG measurement [92]. Mono-polar and bipolar are two types of EEG recording. Mono-polar recording picks up the voltage difference between an active electrode on the scalp and a reference electrode on the ear lobe. Bipolar electrodes give the voltage difference between two scalp electrodes [95].

2.4.1 Electrodes

Usually 10-20 standard electrodes array is used in EEG signal acquisition [93]. This system standardized the location and designation of electrodes on the scalp to provide comprehensive coverage of all regions of the brain [92]. Figure 3 illustrates the Electrode locations of International 10-20 system for EEG recording. Electrodes are labeled with letters and numbers based on the areas that electrodes are placed (Figure 4). Odd numbers are representative for the left side of the subject head and even numbers are representative for right side. Letters are F for frontal area, C for central area, T for temporal area, P for posterior area, and finally O for occipital area [92]. Note that commonly used scalp electrodes consist of Ag-AgCl disks with diameter of 1 to 3 mm and long flexible leads that can be plugged into an amplifier [91].

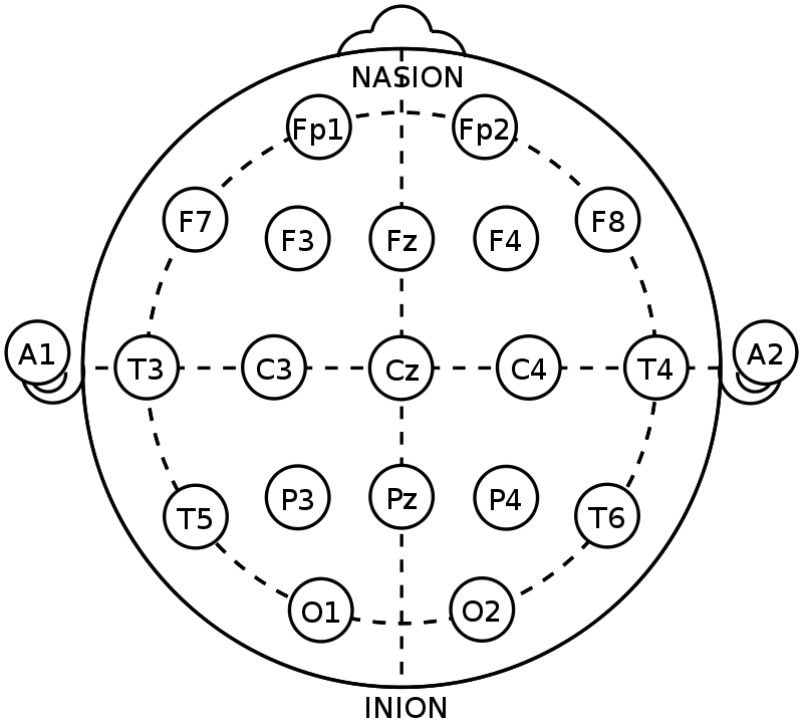

Figure 3: Electrode locations of International 10-20 system for EEG (electroencephalography) recording (Picture form Wikipedia- public domain)

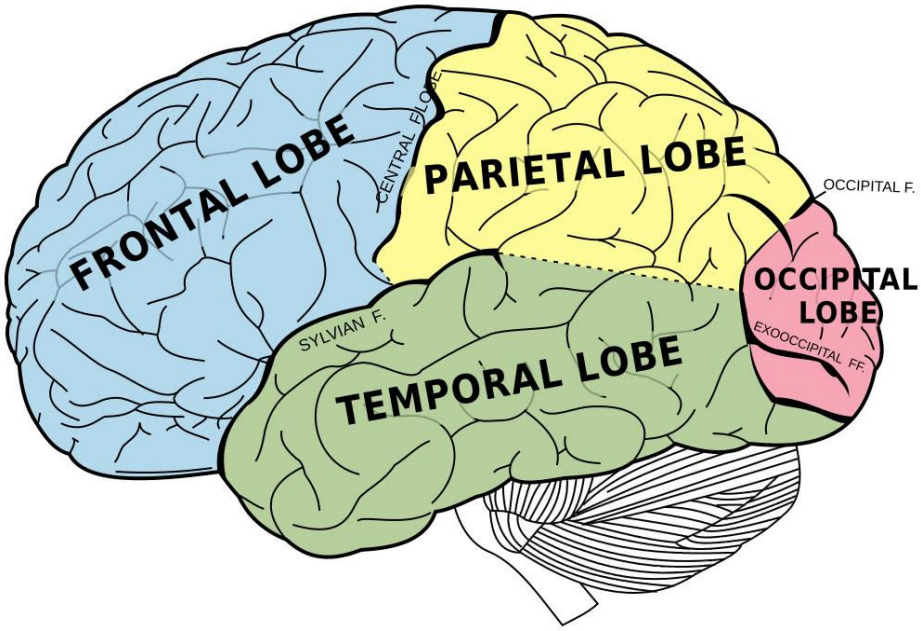

Figure 4: four lobes of the cerebral cortex (Picture source: Public Domain)

2.4.2 Amplifier

The input signal to the amplifier consists of the desired and undesired bio-potentials, harmonics of power line interference signal (50/60 Hz), electrode and tissue interference signals and finally noise and artifacts [92]. Considerable amplifier for high quality EEG recording provides the gain of 106 [91] with high (at least 100MΩ) impute impedance and high (at least 100db) common mode rejection ratio [91, 92].

2.4.3 Filters

Analogue high pass filter with cut-off frequencies range of 0.1 – 0.7 Hz is integrated in amplification unit to reduce the low frequencies coming from bio-electric flowing potentials like breathing. Also a low- pass filter with a cut-off frequency equal to highest frequency of our interest

is used to ensure that the signal is band limited and prevent distortion of signal by interference effects with sampling rate, called aliasing [92]. Digital filtering and digital signal processing techniques can be applied after data are stored in computers.

2.4.4 Converter

Obtained analog signals are repeatedly sampled at a fixed time sampling interval and then are converted to digital by at least 12 bits analogue to digital converters with accuracy lower than over all noise and sampling frequency between 128 - 1024 Hz, to store in computers or recording devices. The smallest amplitude that can be sampled is the base of the converter resolution. The recommended resolution is 0.5 µV [92].

2.4.5 Artefacts

Undesirable electrical potentials which comes from other than brain sources are called artifacts [95]. Artifacts sequences usually have higher amplitude and different shape in comparison to signal sequences. Artifacts in the recorded EEG have two different sources, they may be either patient related like unwanted physiological signals or technical related such as AC power line noise [92].

Any minor body movement, EMG, ECG pulses and pace makers, eye movements and sweeting are some examples for patient related artefacts. However, power 50/60 Hz frequency, impedance fluctuation, cable movement, broken wire contacts, too much electrode jelly or dried pieces and low battery are some examples for technical related artifacts [92].

2.5 EEG Signal Analysis

EEG signals are highly non-Gaussian, non-stationary and have a non-linear and random nature which is usually contaminated by noise and artefacts. The patient's age and their mental status have strong impact on the brain signal characteristics. By using advanced signal processing techniques, important features and hidden information from the signals can be extracted for the diagnosis of different diseases [95].

2.5.1 Signal enhancement and Feature extraction

Signal enhancement or signal pre-processing is applied after EEG signal acquisition. There are several well-known artefact removal techniques with different advantages and disadvantages for particular purpose of uses.

In order to diagnosis a disease the feature extraction methods are applied to extract essential information from noise-free EEG signals which obtained after applying the signal enhancement techniques. Methods such as Fast Fourier Transformations (FFT), Principal component analysis (PCA), Independent Component Analysis (ICA), Wavelet Transformations (WT), Wavelet Packet Decomposition (WPD) are methods that can be used to extract signal features. Among these ICA, PCA, WT, WPD, FFT are mostly used [93].

Independent Component Analysis (ICA) feature extraction method forms the components that are independent to each other. This method helps in noise separation from EEG signal [93]. Principal Component Analysis (PCA) also uses as feature extraction method. The principal components of all-time series channels can be extracted by PCA method. It is a powerful tool for analyzing and for dimension reduction of data without losing of information. Wavelet transformation is a multi-resolution analysis that can act as low pass filter as well as high pass filter and it is able to extract

dynamical Information from EEG signals both in time and frequency domain. Wavelet Packet Decomposition (WPD) can extract features in both time and frequency domain from non-stationary signals with the coefficients mean of WT [93]. This method needs more computational time. And finally Fourier Transform, which extracts the signal features by transforming the signals from the time domain to the frequency domain. This method is suitable to transform the stationary signals and linear random processes. It is very sensitive to noise and it cannot measure both the time and frequency [93].

2.6 Coma

Coma is defined as a state of unconsciousness that patient does not have any respond to the sensory or physical stimuli. A person in a state of coma is described as being comatose**.** A wide range of conditions may be associated with coma or impaired consciousness such as traumatic brain damage, hypoglycemia and drug overdose [98].

Glasgow coma scale (GCS) and other Clinical scales like motor responsiveness, verbal performance, and eye opening are used for assessing the depth and duration of impaired consciousness and coma [98].

2.7 Cardiac Arrest (CA)

Sudden cardiac arrest can be triggered by an electrical malfunction (arrhythmia) in the heart. A common arrhythmia in cardiac arrest is ventricular fibrillation. During the cardiac arrest blood cannot be pumped to the vital organs such as Brain and this causes consciousness loss on patients. Performing cardiopulmonary resuscitation (CPR) or using defibrillator device can restore the normal heart rhythm within minutes after CA [99].

2.8 Therapeutic hypothermia

Therapeutic hypothermia is an advanced treatment to improve neurologic outcome after cardiac arrest. The early studies focused on moderate hypothermia but hypothermia with target temperatures of 32–34°C was the main focus on later studies. Cooling down the body temperature of cardiac arrest patients to 32°C to 34°C for 12 to 24 hours when the initial rhythm was ventricular fibrillation is recommended by The International Liaison Committee on Resuscitation [100].

Therapeutic Hypothermia has three main phases (Figure 5): Cooling (~4 hours) to get the patient to target body temperature, Hypothermia (~24 hours) to maintain the patient's temperature within the target range (32° to 34° C) and controlled rewarming (~12 to 16 hours).

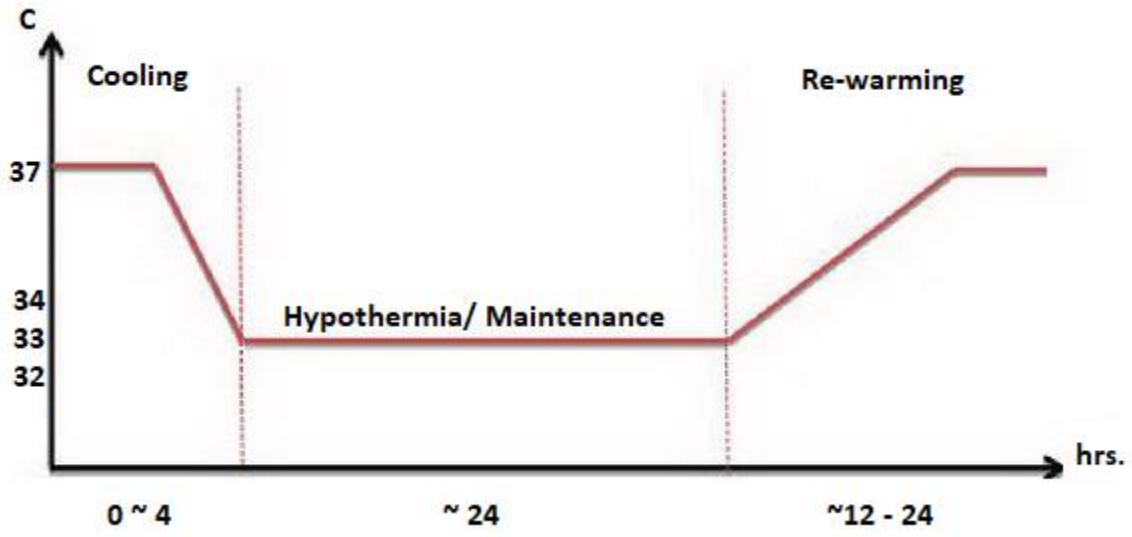

Figure 5: Therapeutic Hypothermia phases

2.9 Cardiac Arrest and Hypothermia:

Neurological complications after cardiac arrest (CA) can be fatal. Hypothermia treatment has been shown to be beneficial for CA patients. But understanding the mechanism and establishing neurological outcomes remains challenging because effects of CA and hypothermia are not well characterized [101]. Electroencephalogram (EEG) monitoring in patients treated with therapeutic hypothermia after cardiac arrest may assist in early outcome prediction [97].

CHAPTER 3: LITERATURE REVIEW [118]

3.1 *Introduction*

The aim of this review is to discuss the State-of-the-Art in employment of quantitative measures of EEG for prediction of the outcome in CA subjects treated with hypothermia. The review can provide a platform for the future potential development and examine of new measures and/or methods for the early and accurate CA outcome prediction for the patients undergoing hypothermia.

3.2 Materials and methods

Pubmed database was searched for the articles which were published between year 2000 and the present time (August 2017) using (logical conjunction of) the following keywords:
"quantitative EEG" and "cardiac arrest" and "hypothermia". In our review, we considered both animal and human studies.

The previous investigations on the effect of changes in temperature of the brain have indicated that hypothermia has relatively similar influences on EEG in animals and humans [29]. The search resulted in more than 40 publications. The abstracts of these publications (and the body of the papers if the abstracts did not provide sufficient information) were studied to verify the relevancy of each paper to the subject of our search (employing quantitative measures of EEG for automatic CA outcome prediction in subjects undergoing hypothermia). Following exclusion of the irrelevant publications, remaining papers were read carefully, their proposed measures were identified and their results were summarized.

3.3 Results

Exclusion of the irrelevant papers (those not related to employment of quantitative measures of EEG, or not related to cardiac arrest or hypothermia) resulted in selection of 24 papers. Table 1 lists the selected papers along with a summary of the main findings of the papers. Table 2 includes a list of quantitative measures (features) of EEG which have been employed in prediction of CA outcome for the subjects undergoing hypothermia. For simplicity, the identified measures were grouped into four groups: conventional entropy based measures; burst suppression measures; information quantity measures; and combined measures. In the following subsections, we go over the definition of each measure and discuss its efficacy in prognostication of CA outcome for hypothermia subjects.

Table 1: List of selected publications along with a summary of their results (ordered based on the year of publication)

Paper, Year , Subject	EEG feature and how it was obtained	Summary of results
Jia et al. [25] 2006 28 rats	Information quantity (IQ), EEG was measured using DI700 Windaq (Data Q Instruments, Akron, OH), and its feature was extracted with in-house software	The 72-h NDS of the hypothermia group was significantly improved compared to the normothermia. The IQ showed significantly different values between hypothermia and normothermia groups. There was a trend toward minor metabolic acidosis in the normothermic controls compared to hypothermic rats with a slight but statistically significant difference in bicarbonate concentration at 40 min post-CA
Shin et al. [49] 2006 30 rodents	Information quantity (IQ), EEG was measured using DI700 Windaq (Data Q Instruments, Akron,	The IQ was greater for hypothermic than

Paper, Year , Subject	EEG feature and how it was obtained	Summary of results
	OH), and its feature was extracted with in-house software	normothermic rats, with a difference of more than 0.2
Jia et al. [19] 2008 28 male Wistar rats	Information quantity (IQ), EEG was measured using DI700 Windaq (Data Q Instruments, Akron, OH), and its feature was extracted with in-house software	Greater recovery of the IQ was found in rats treated with hypothermia, compared to normothermia and hyperthermia. IQ values correlated strongly with 72-h NDS as early as 30 min post-CA (correlation = 0.735)
Lu et al. [44] 2008 12 Wistar rats	C0 Complexity, EEG was measured using DI700 Windaq (Data Q Instruments, Akron, OH), and its feature was extracted with in-house software	Significantly greater C0 complexity was found in hypothermic group than that in normothermic group as early as 4-h after the ROSC. C0 complexity at 4-h correlated well with the 72-h NDS (correlation = 0.882)
Shin et al. [50] 2008 13 rats	Subband information quantity (SIQ), and information quantity (IQ). EEG was measured using DI700 Windaq (Data Q Instruments, Akron, OH), and its features were extracted with in-house software	During hypothermia, SIQ was more correlated with neurological outcome than IQ (correlation of 0.74 vs. 0.65)
Jia et al. [51] 2008 36 rats	Subband information quantity (SIQ), EEG was measured using DI700 Windaq (Data Q Instruments, Akron, OH), and its feature was extracted with in-house software	The 72-h NDS of the immediate hypothermia (IH, immediately post-resuscitation maintained for 6-h) group was significantly better than the conventional hypothermia (CH, starting 1 h post-resuscitation, maintained 12 h) group. The SIQ values of the IH group was significantly higher. The neuronal cortical activity (measured by Cresyl violet staining) of the IH group was significantly lower. PCO2 was significantly lower and

Paper, Year , Subject	EEG feature and how it was obtained	Summary of results
		blood pressure was significantly in IH at 40 min post-CA
Kang et al. [26] 2009 10 Wistar rats	Multi-scale entropy (MSE), EEG was measured using DI700 Windaq (Data Q Instruments, Akron, OH), and its feature was extracted with in-house software	Alpha-rhythm MSE measured within 1–2.5-h post-CA was significantly different between the hypothermic and normothermic groups
Wennervirta et al. [21] 2009 30 comatose patients	Burst suppression ratio (BSR), Wavelet subband entropy (WSE), response entropy and state entropy. EEG was measured using (Datex-Ohmeda S/5, GE Healthcare, Helsinki, Finland). Wavelet subband entropy (WSE) was extracted by in-house software. Burst suppression ratio (BSR), response entropy and state entropy were obtained by Datex-Ohmeda entropy module	In the patients with good outcome (CPC of 1 and 2), BSR, WSE, response entropy and state entropy were all significantly higher. However, neuron-specific enolase, protein 100B, and pulsatility index of cerebral blood flow velocity were significantly lower in patients with good outcomes
Leary et al. [61] 2010 62 patients	Bispectral Index (BIS), BIS monitoring (Aspect Medical Systems, Norwood, MA, USA)	BIS was significantly higher in the good outcome group. BIS at 24 h post-CA was the best predictive of CPC 1–2 outcome compared to the other time points; a BIS cut-point of 45 exhibited a sensitivity of 63% and a specificity of 86%, with a positive likelihood ratio of 4.67
Seder et al. [60] 2010 97 patients	Bispectral Index (BIS) BIS monitoring (Aspect Medical Systems, Norwood, MA, USA)	The BIS was higher in patients with good outcome (37 [28–40] vs. 7 [3–15]). BIS < 22 predicted poor outcome with a likelihood ratio of 14.2 and accuracy of 0.91

Paper, Year , Subject	EEG feature and how it was obtained	Summary of results
Chen et al. [33] 2013 20 male Sprague–Dawley rats	Burst suppression frequency (BSF), and spectrum entropy (SE). EEG was measured using DI700 Windaq (Data Q Instruments, Akron, OH), and features were extracted with in-house software	96-h NDS and survival were significantly better in the hypothermic group. BSF and SE were greatly improved in the hypothermic group and correlated with 96-h NDS and survival
Stammet et al. [64] 2013 75 patients	Bispectral Index (BIS), Quatro sensor from ASPECT Medical Systems Inc., Newton, MA, USA	NSE and S100B levels were significantly lower and BIS values were significantly higher in patients with good outcome (CPC 1–2). Patients with S100b level above 0.03 mg/l and BIS below 5.5 had a 3.6-fold higher risk of poor neurologi- cal outcome. S100b and BIS predicted 6-month mortality (log-rank statistic: 50.41)
Riker et al. [62] 2013 509 patients	Bispectral Index (BIS), models A2000 and VISTA from Covidien Medical, Boston, MA, USA	Patients who awakened early had higher BIS values after the first dose of neuro -muscular blockade
Tjepkema et al. [54] 2013 109 patients	Cerebral Recovery Index (CRI), EEG was measured using Neurocenter (Clinical Science Systems, Voorschoten, The Netherlands) and its feature was extracted with in-house software	CRI at 24-h post-CA classified the good outcome (CPC 1–2) versus poor outcome (CPC > 2) with specificity of 100%
Selig et al. [63] 2014 79 patients	Bispectral Index (BIS), A-2000 system XP, software version 3.30, Aspect Medical Systems Company, Newton, Massachusetts, USA and the BIS-Quattro sensor electrodes	Using BIS < 40 as threshold criteria, poor neurological outcome was predicted with a specificity of 89.5% and a sensitivity of 85.7%. The odds ratio for predicting a poor outcome was 0.921 (95% CI 0.853–0.985)

Paper, Year , Subject	EEG feature and how it was obtained	Summary of results
Noirhomme et al. [28] 2014 46 comatose patients	Burst Suppression Ratio (BSR) and Approximate Entropy (AE). EEG was measured using Viasys Neuro-care, Madison, WI and its feature was extracted with in-house software	BSR was significantly lower and AE was significantly higher in patients with good outcome (CPC 1–2)
Ghassemi et al. [10] 2014 167 patients	Cerebral Recovery Index (CRI), and Enhanced Cerebral Recovery Index (ECRI) EEG was measured with standard 10–20 montage (no further info is provided) and its features were extracted with in-house software	Relative to CRI, ECRI measured in 24-h post-CA increased the classification accuracy of good outcome (CPC 1–2) versus poor outcome classification by an average of 27%
Seder et al. [48] 2014 171 patients	Bispectral Index (BIS), models A2000 and VISTA from Covidien Medical, Boston, MA, USA	BISi < 10 suffered 82% neurological-cause and 91% overall mortality, BISi 10–20 suffered 35% neurological and 55% over-all mortality, and BISi > 20 suffered 12% neurological and 36% overall mortality
Stammet et al. [65] 2014 75 patients	Bispectral Index (BIS), Quatro sensor from ASPECT Medical Systems Inc., Newton, MA, USA	BIS was significantly higher in good outcome (CPC 1–2). Analysis of BIS recorded every 30 min provided an optimal prediction after 12.5 h, with an accuracy of 0.89
Deng et al. [52] 2015 14 rats	Subband information quantity (SIQ), and information quantity (IQ). EEG was measured using DI700 Windaq (Data Q Instruments, Akron, OH), and features were extracted with in-house software	Both IQ and SIQ at as early as 1-h post-CA had high correlation (0.8) with 72-h NDS score. IQ could identify the presence of high-frequency oscillations during the recovery from severe brain injury
Deng et al. [53] 2015	Subband information quantity (SIQ), EEG was measured using DI700 Windaq (Data Q Instruments, Akron,	The Gamma-band SIQ had the strongest correlation (between 0.52 and 0.78), while Delta-band SIQ had the lowest correlation to 72-h NDS score

Paper, Year , Subject	EEG feature and how it was obtained	Summary of results
24 Wistar rats	OH), and its features was extracted with in-house software	Better recovery of Gamma-band SIQ was found in the hypothermia group com- pared with the normothermia group and hyperthermia group
Moshirvaziri et al. [18] 2016 11 comatose patients	Wavelet subband entropy (WSE), EEG was measured using Viasys Neuro-care, (Madison, WI) and its feature was extracted with in-house software	WSE over the frequency range of 64–100 Hz captured from the inferior frontal lobes were significantly higher in those survived
Jouffroy et all [66] 2017 46 patients	Bispectral Index (BIS), (BIS monitor – Covidien©) No further info is provided	BIS values were significantly lower in those who died (4 versus 34)
Ochiai et al. [67] 2017 103 patients	Bispectral Index (BIS), A-2000 and BISx monitors for different years both from Aspect Medical Systems, MA, USA	Low mean BIS value best predicted poor outcomes with CPC of 3 to 5 with an accuracy of 0.861

3.3.1 Conventional entropy-based measures

In information theory, Shannon entropy is defined as a measure of the uncertainty in a random variable *X* by quantifying the expected value of the information contained in a signal [30]. Entropy is typically measured in bits as

$$Shannon\ Entropy = -\sum_{i}^{N} p_i \log_2 p_i, \qquad (1)$$

where p_i is the probability of random variable X being equal to value X_i for $i = 1, 2, ..., N$. Note that $\sum_{i=1}^{N} p_i = 1$. A higher level of randomness or complexity in the data generally indicates larger entropy values.

Similar to many other organs, brain can be considered as a system with high level of complexity (entropy). A reduction of biological system's complexity is often interpreted as a pathological or deteriorating state [31]. Brain injury and the disruption of its normal functionality can result in the reduction of brain's complexity [32]. Therefore, using an appropriate EEG entropy analysis, one may be able to track the brain's recovery progress after brain injury. Several conventional entropy-based measures have been proposed for the CA outcome prediction. Here, we review the definition of those which have shown efficacy in prediction of the outcome when the subject went under hypothermia treatment.

3.3.1.1 Spectrum entropy

The spectrum entropy (*SE*) of the EEG signal is calculated as the Shannon entropy of the normalized energy of the signal within certain frequency subbands of interest. In other words, the probability *pi* in Eq. (1) is defined as:

$$p^i = \frac{E_i}{\sum_{i=1}^{N} E_i}, \qquad (2)$$

where *Ei* is the energy of the signal within *i*th subband calculated from power spectral analysis of the EEG signal.

Chen et al. choose $N = 4$ frequency subbands to study the efficacy of *SE* as a prognostic measure of CA outcome in rats: Delta (0.5–4 Hz), Theta (4–8 Hz), Alpha (8–13 Hz), and Beta (13–30 Hz) [33]. The results of this study indicated that the hypothermic rats have significantly higher values of *SE* (and better neurological outcome) relative to normothermic controls. Using a logistic regression analysis, the authors also showed that *SE* value at 6-h after restoration of spontaneous circulation (ROSC) was an independent predictor of 96-h survival outcome in hypothermic group. Two spectrum entropy-based variables that can be measured using a commercially available product (Datex-Ohmeda entropy module, GE Healthcare, Helsinki, Finland) are response entropy and state entropy [22]. State entropy is the entropy of the normalized energy of the signal over the EEG-dominant frequency range of 0.8–32 Hz, indicating the effect of hypnotics on the cortex. On the other hand, response entropy is the spectrum entropy over the frequency range of 0.8–47 Hz (including EEG and facial electromyography frequency components) and can be used to detect the patient's responsiveness [21, 22]. In a study of 30 comatose patients by Wennervirta et al., both relative entropy and state entropy demonstrated significantly higher values during the first 24 h after CA in patients with cerebral performance category (CPC) [34] of 1 or 2 comparing to the other patients [21].

3.3.1.2 Approximate entropy

Approximate entropy (*ApEn*) is a parameter that quantifies the unpredictability of fluctuations in a time series [35]. Since its introduction two decades ago, *ApEn* has been widely used to characterize the complexity of various biological and physiological data [36]. *ApEn* is defined as the negative natural logarithm of the probability that the data sequences within a time series that are close for *m* points remain close for an additional point (*m* + 1 points).

For an EEG signal $\{s(i) \mid i = 1,2,...,N\}$, one can define a template vector $\mathbf{X}_m(i)$ as:

$$\mathbf{X}_m(i) = \{s(i+k) \mid 0 \le k \le m-1\}. \tag{3}$$

Note that there exist $N-m+1$ of such vectors where $1 \le i \le N-m+1$. Now, let us assume that the distance between two vectors $\mathbf{X}_m(i)$ and $\mathbf{X}_m(j)$ is the maximum difference of their corresponding scalar components:

$$d(\mathbf{X}_m(i), \mathbf{X}_m(j)) = \max(|s(i+k) - s(j+k)|), \tag{4}$$

Where $0 \le k \le m-1$. Vector $\mathbf{X}_m(j)$ with $1 \le j \le N-m+1$ is called a match for template $\mathbf{X}_m(i)$, if $\mathbf{X}_m(j)$ is less than r distance away from $\mathbf{X}_m(i)$, i.e., when $d(\mathbf{X}_m(i), \mathbf{X}_m(j)) < r$.

Thus, the probability that vector $\mathbf{X}_m(j)$ is within r distance of $\mathbf{X}_m(i)$ can be calculated as:

$$C_i^m(r) = \frac{n_{im}(r)}{N-m+1}, \tag{5}$$

where $n_{im}(r)$ is the number of matches for template $\mathbf{X}_m(i)$. By averaging all $C_i^m(r)$ as:

$$C_m(r) = \frac{1}{N-m+1} \sum_{i=1}^{N-m+1} C_i^m(r), \tag{6}$$

we can calculate *ApEn* for EEG signal of finite length N, with pattern length m and similarity criterion r, as:

$$ApEn = \log_e \frac{C_m(r)}{C_{m+1}(r)}. \quad (7)$$

Noirhomme et al. employed *ApEn* measure with m = 2, r = 1.4, and 8-s epochs to study the prognostic value of this parameter in 46 comatose patients in hypothermia [28]. The results revealed that the average *ApEn* value measures during hypothermia was significantly higher in patients with good outcome whose CPC values are 1 or 2.

3.3.1.3 Multiple scale entropy

A signal complexity is in general a "meaningful structural richness" [37] that incorporates correlations over multiple spatiotemporal scales [38]. While the previously discussed measures of entropy quantify the regularity of time series on a single scale, multiple scale entropy (*MSE*) considers the complexity of the signal over multiple scales. Given the clinical significance of various frequency subbands in EEG analysis, *MSE* may be a more appropriate measure for CA outcome prediction.

For an EEG signal $\{s(i) \mid i = 1,2,...,N\}$, *MSE* of the signal is calculated in two steps: For a given scale (λ), first a moving-average filtering (with zero percent overlapping) is applied to the data to obtain a "coarse grained" signal y_j^{λ} as

$$y_j^{\lambda} = \frac{1}{\lambda} \sum_{i=(j-1)\lambda+1}^{j\lambda} s(i), \qquad (8)$$

where $1 \le j < \frac{N}{\lambda}$. Then, the sample entropy (a refined version of *ApEn* which excludes self-matching to reduce the estimator's bias [39]) of each coarse-grained signal is calculated. The final *MSE* is obtained as a plot of the calculated sample entropies over a range of potential scale values $\lambda = 1, 2, ..., .$

As synchronous activity in thalamic pacemaker cells are related to the α-rhythm [40], Kang et al. hypothesized that the complexity changes of EEG *α*-rhythms (measured by *α*-rhythm *MSE*) may reveal different degrees of brain recovery during hypothermia after CA [26]. Given the sampling frequency of the signal, the scaling factors corresponding to the Alpha band (8–12 Hz) were identified and the values of *MSE* over those scales were averaged and used as the *α*-rhythm *MSE* measure. The results of this study on rodents showed that *α*-rhythm *MSE* measure within 1–2.5 h post-CA was significantly different between the hypothermic and normothermic groups. Furthermore, the authors found that good recovery outcomes were always achieved, when the ratio of *α*-rhythm *MSE* measured at 3-h post-CA to that of the baseline (before-CA) was above 0.85. In that study, the good outcome was defined as a case where the neurological deficit scale (NDS) was above 60. Note that NDS is a neurological outcome evaluation standard which includes sub-scores of general behavioral deficit, brain-stem function, motor and sensory assessment, behavior, and seizures [41, 42].

3.3.1.4 Wavelet subband entropy

Discrete Wavelet transform is one of the most efficient tools for the denoising of the transients, non-stationary and aperiodic signals such as EEG with low redundancy and computational complexity.

To calculate Wavelet subband entropy (*WSE*), one needs to first apply a *L*-level discrete wavelet transform to the signal. The value of *L* is usually determined based on the sampling frequency and the clinical subbands of interests. Let us assume that $\Im_i^l$ is i^{th} wavelet coefficient at level *l*, where $l = 1, 2, ..., L$. Then, the *l*-level *WSE* can be obtained as the Shannon energy of the squared and normalized version of the coefficients at that decomposition level. In other words,

$$WSE^l = -\sum_{i=1}^{N} p_i^l \log_2 p_i^l \qquad \text{where} \qquad p_i^l = \frac{(\Im_i^l)^2}{\sum_{i=1}^{N} (\Im_i^l)^2}. \tag{9}$$

Wennervita et al. employed *WSE* calculated over Beta subband (16–32 Hz) using Daubechies 3 mother wavelet to study the CA outcome for the patients undergoing hypothermia [21]. Their result indicated that Wavelet Beta subband entropy measured between 24 and 48 h post-CA was significantly higher in the good outcome group (CPC of 1–2) evaluated within a 6-month follow-up period.

In a recent study, our group analyzed a dataset of 16-channel EEG signals collected from 11 CA patients undergoing hypothermia at Long Beach Memorial Medical Center using *WSE* [18]. Our results revealed that the frequency oscillations between 64 and 100 Hz captured from the inferior frontal lobes are significantly more complex in the CA patients who survived.

3.3.1.5 C0 complexity

Another robust measure of the signal's complexity is C0, a percentage of stochastic components of the signal [43]. For an EEG signal $\{s(i) \mid i = 1, 2, ..., N\}$, C0 complexity is defined as:

$$C0 = \frac{\sum_{i=1}^{N} |s(i) - y(i)|^2}{\sum_{i=1}^{N} |s(i)|^2} \quad (10)$$

where $\{y(i) \mid i = 1, 2, ..., N\}$ is obtained from EEG signal by zeroing the signal at all frequency components where the power of the signal is lower than the signal's average power.

Lu et al. employed C0 complexity to analyze the nonlinear characteristic of EEG for prediction of the outcome in 12 Wistar rats who were randomly undergoing hypothermia and normothermia [44]. Significantly higher C0 complexity values were found in hypothermic group (relative to normothermic group) as early as 4 h after the ROSC. Furthermore, C0 complexity at 4-h post-ROSC was strongly correlated with the 72-h NDS (correlation = 0.882).

3.3.2 Burst suppression measures

Burst suppression is characterized by the presence of periods of bursting, when EEG amplitude rises above certain threshold typically in the range of 75–250 μV, followed by long periods (at least 0.5 s) of suppression, when EEG shows low amplitude activities (typically below 10 μV) [45, 46]. A clear description of an algorithm to automatically detect the burst suppression patterns in EEG signal has been provided by Sarkela et al. in [47]. Several burst suppression features can be used to quantify the EEG background activities, e.g., burst suppression ratio (BSR), and burst suppression frequency (BSF).

3.3.2.1 *Burst suppression ratio*

BSR is defined as the ratio between the total suppression time and total recording time [28]. There are commercially available products that can be used to obtain BSR values. Datex- Ohmeda entropy module (from GE Healthcare, Helsinki, Finland) calculates BSR using the algorithm described in [22] for every 1 min of data, while Bispectral Index (BIS) monitors (from ASPECT medical systems Inc., MA, U.S.A) obtains BSR for every 63 s of data using a proprietary algorithm [48].

A study on 30 comatose CA patients treated with induced hypothermia revealed that BSR (measured by Datex-Ohmeda entropy module) during the first 48 h after CA was significantly lower in patients with good outcomes (CPC of 1–2) evaluated within a 6-month follow-up period [21]. Similarly, in another study on 46 CA patients, low BSR values (computed with a software developed in house) were associated with good neurological outcome (CPC of 1–2) evaluated at 3-month post-CA [28].

3.3.2.2 *Burst suppression frequency*

BSF is a measure of frequency content of bursts (during burst suppression periods), and can be easily obtained using spectral analysis [33]. Chen et al. found that BSF was significantly Journal of higher in hypothermic rats compared to the control groups. The observed continuous increasing trend of BSF during the first 2 h after resuscitation of rats treated with hypothermia showed the effectiveness of therapeutic hypothermia in brain recovery. This study also indicated that the 2-h post-ROSC BSF value was independently predictive of 96-h survival outcome.

3.3.3 Information quantity measures

3.3.3.1 Information quantity

Information Quantity (*IQ*) measure was developed based on the assumption that a better neurological outcome is associated with larger information content of the brain rhythm [49].

IQ is defined as time dependent Shannon entropy of decorrelated EEG signals using discrete wavelet transform (DWT).

A sliding temporal window $W(n, w, \Delta)$ is applied to the EEG signal $\{s(i) \mid i = 1, 2, ..., N\}$ such that:

$$W(n,w,\Delta)=\{s(i)\,|\,i=1+n\Delta,...,1+w\Delta\} \tag{11}$$

where w is the length of sliding window, Δ is the sliding step, and $n=0,1,...,\frac{N}{\Delta}-w+1$. Then using a r-level DWT, the signal within each window is decomposed into frequency subbands that represent standard clinical bands of interest. The DWT coefficients of each window, $WC(r, n, w, \Delta)$, are obtained and the time dependent *IQ* is calculated as:

$$IQ(n)=-\sum_{m=1}^{M} p_m(n)\log_2(p_m(n)), \tag{12}$$

where $pm(n)$ is the probability that the sampled signal belongs to the interval $\{Im : m = 1, 2, ...,M\}$ and is obtained as the ratio between the number of the samples found within interval *Im* and the total number of samples in $WC(r, n, w, \Delta)$.

IQ has demonstrated a superior tracking capability for both frequency changes and dynamic amplitude change comparing to conventional entropy-based measures such as Shannon entropy and Wavelet entropy.

In a study of 28 rats, the *IQ* values showed significantly difference between hypothermia and normothermia groups [25]. Also, the experiments carried out on 30 rodents indicated that brain injury results in a reduction of *IQ* values [49]. Furthermore, the hypothermic rats showed greater average *IQ* than normothermic rats for various injury levels, confirming that hypothermia accelerates brain's electrical recovery after CA. In another study of 28 rats, *IQ* values at 30-min post-CA also showed a strong correlation with 72-h NDS [19]. These results demonstrate the efficacy of the *IQ* at prognostication of CA outcome for hypothermia.

3.3.3.2 Subband information quantity

As discussed in Sect. 4.3.3.1., *IQ* measures information of the gross EEG signal in all frequency bands from delta to gamma. However, brain recovery from CA may be more related to the activities of individual EEG subbands. In fact, a more recent study on rats indicated that *IQ* prognostication sensitivity may degrade over time by overestimating the CA outcome at later period of recovery [50]. In contrast to *IQ*, subband information quantity (*SIQ*) calculates the information content within each *k* th subband of a *r*-level DWT separately:

$$SIQ^k(n) = -\sum_{m=1}^{M} p_m^k(n)\log_2(p_m^k(n)), \qquad (13)$$

where $k = 1,2,...,r+1$. Note that $p_m^k(n)$ is the probability that the sampled signal in k^{th} subband belongs to the interval $\{I_m : m = 1,2,...,M\}$, and it is obtained as the ratio between the number of the samples found within interval I_m and the total number of samples in k^{th} subband.

Then the overall *SIQ* is calculated by averaging the individual subband information quantities over all subbands of interests:

$$SIQ(n) = -\sum_{k=1}^{r+1} SIQ^k(n). \qquad (14)$$

The examination of *IQ* and *SIQ* trends in a rodent hypothermia study indicated that *SIQ* values were more highly correlated (correlation of 0.74 vs. 0.65) with 72-h post-CA NDS than *IQ* values. It was also revealed that the most significant variations of *SIQ* were contributed by Theta, Beta, and Alpha bands.

Another study on 36 rats showed that the *SIQ* value was significantly higher when hypothermia was administered immediately post-resuscitation and maintained for 6-h relative to when hypothermia started 1 h post-resuscitation and maintained 12 h [51]. Also in a study of 14 rats, Deng. et al. showed that both *IQ* and *SIQ* at 1-h post-CA had high correlation (0.8) with 72-h NDS scores [52].

In another study of 27 rats by the same group, the Gammaband *SIQ*values showed the highest correlation with 72-h NDS at every time point from 30-min to 72-h post-ROSC, while the Delta-band *SIQ* showed the lowest correlation to the CA outcome [53].

3.3.4 Combined measures

3.3.4.1 Cerebral recovery Index

Given the promising results of CA outcome predictions using single quantitative EEG measures (features), one could possibly enhance the accuracy in prognostication by using a combination of multiple features. Within this context, Tjepkema - Cloostermans et al. employed a set of EEG

features to define a single number index, called cerebral recovery index (*CRI*), for the prognostication of outcome in CA patients treated with hypothermia [54]. Motivated by the criteria generally employed by the neurologists for visual inspection of EEG patterns, the authors chose the following five EEG features:

- *SD*: Standard deviation of the EEG signal over 5-min epochs were used as a measure of the signal power.
- Hsh: Shannon entropy of the signal was calculated where the values of pi in Eq. (1) were determined using a histogram of the amplitude of the signal with 1 μV bin-width over the range of (− 200 to 200 μV).
- ADR: The EEG signal ratio between Alpha-band (8–13 Hz) and Delta-band (0.5–4Hz) was obtained from power spectrum analysis of the signal.
- COH: The mean coherence in the Delta-band between all possible combinations of EEG channels was used as a measure to quantify EEG patterns with abnormally high synchronization level.
- REG: Finally, to differentiate burst suppression from continuous EEG patterns, a new regularity measure (REG) was introduced. For this purpose, first a non-negative smoothed version of the EEG signal was obtained by applying a 0.5-s moving-average filtering to the square of the signal

  {s2(i)_i = 1, ..., N} . Then the values of the smoothed signal were sorted in descending order (let us call this sorted smoothed signal as {q(i)_i = 1, ...N}) and the normalized standard deviation of the sorted values was calculated as

$$REG = \sqrt{\frac{\sum_{i=1}^{N} i^2 q(i)}{\frac{1}{3} N^2 \sum_{i=1}^{N} q(i)}} \tag{15}$$

REG range of values is between 0 and 1. An EEG signal with shorter bursts would result in smaller values of REG, while values closer to 1 indicate a signal with longer bursts.

Following the calculation of above features, they were normalized using a sigmoidal transform function whose coefficients were selected heuristically [10]. Given the significance of the role of the EEG signal power (*SD*) as an indicator of brain's recovery, the cerebral recovery index was defined as:

$$CRI = \frac{SD(H_{sh} + ADR + COH + REG)}{4}. \tag{16}$$

The study of 109 hypothermic CA patients showed that the calculated *CRI* at 24-h post-CA can differentiate the dichotomized good outcome (CPC score of 1 or 2) versus poor outcome (CPC score of above 3) with the following accuracies: $CRI < 0.29$ predicted the poor outcome with sensitivity of 55% and specificity of 100%, while $CRI > 0.69$ predicted the good outcome with sensitivity of 25% and specificity of 100%.

3.3.5 Enhanced cerebral recovery index

In a recent study, Ghassemi et al. [10] introduced an enhanced version of cerebral recovery index (*ECRI*) by including the following additional features:

- Tsalis entropy area (TsEnA): Tsalis entropy is a non-extensive statistics to quantify the regularity of a signal [55], and is defined as

$$TsEn = \frac{1-\sum_{i=1}^{N}(p_i)^q}{1-q}, \tag{17}$$

where q is the nonextensivity degree. Comparing to conventional measures of entropy, TsEn can better describe the quasi-stationary properties of weakly ergodic systems in long-ranging interactions [55]. Since EEG signal is the result of long-ranging interactions across corticothalamic and thalamocortical networks [56], in general, TsEn may be able to provide more detailed information on EEG spikes and bursts, relative to other traditional entropy measures.

To predict the CA arrest outcomes in a rodent model (with no hypothermia), Zhang et al. defined a new Tsalis entropy-based measure named Tsalis entropy area (TsEnA) to quantify the complex dynamics of burst suppression in EEG after CA [57]:

$$TsEnA = \sum_{t_1}^{t_2} \frac{N^{1-q}+\sum_{i=1}^{N}(p_i)^q}{1-q} \quad \text{for } q \neq 1 \tag{18}$$

where t1 and t2 are the starting and ending times of burst suppression. Using a smooth histogram of the amplitude of the signal with N = 50, and q = 3, the authors achieved a high correlation of 0.86 between TsEnA values and 72-h post-ROSC NDS scores. Given the success of this study, Ghassemi et al. used TsEnA with q = 2 as one of the features to predict CA outcome in patients undergoing hypothermia.

- Cepstrum coefficients (CP) is the inverse of the Fourier transform of the log-magnitude of the spectrum of the signal [58]. CP provides information about rate of change in different spectrum bands and is widely used as a feature vector in signal processing.

- Maximum phase lag index (PLI_{Max}) across all EEG channels was used as a measure of connectivity/synchronization. It is known that the phase lag index characterizes the asymmetry of the distribution of phase differences $\Delta\phi$ between two signals [59] and can be calculated as

$$PLI = \left| < Sign[\Delta\phi(t_i)] > \right|, \tag{19}$$

where $\{t_i \mid i = 1,\ldots,N\}$ are the time indices. PLI is within the range of zero to one. A value of zero indicates either no coupling or coupling with $\Delta\phi$ centered around $0 \bmod \pi$, while a value of one means phase locking at a $\Delta\phi$ different than $0 \bmod \pi$. .Ghassemi et al. used the maximum values of PLI over all EEG channels as one of the additional features for CA outcome prediction.

- A binary low voltage state measure to detect the EEG less than 1 μV.

A logistic regression model was applied to the aforementioned EEG features to obtain the enhanced cerebral recovery index (*ECRI*) and to estimate a dichotomized CPC score at discharge (CPC scores of 1–2 vs. CPC scores of 3–5). A one-leave-out cross-evaluation of the proposed method on EEG data of 167 CA patients spanning from three institutions revealed that (comparing to *CRI*) the *ECRI* increased the accuracy of prognostication in the first 24-h post-CA by an average of 27%.

These results confirm the efficacy of employing the combined features in prognostication of CA outcome for the patients undergoing the hypothermia.

3.3.5.1 Bispectral Index

Bispectral index (BIS) is a quantitative measure of EEG that is measured by a commercially available device from ASPECT Medical Systems Inc., MA, USA. The first version of the product entered the market in 1994, and since then BIS monitors have undergone various updates both in terms of software and hardware. Frontotemporal adhesive sensors are used to capture the surface EEG, then a weighted sum of several EEG features are obtained (including frequency below which 95% of the power spectrum resides, the relative beta ratio, BSR, and a measure of EEG phase coupling), and then a number in the range of 0–100 is reported to indicate the level of awareness [48]. BIS is simple to apply, however the exact algorithm to calculate the index is proprietary information. In fact, the use of BIS monitors to track the hypnotic component of anesthesia has been controversial at times [45].

Several recent studies have been able to use BIS for the prediction of CA outcome for the patients undergoing hypothermia. The majority of these studies have revealed that the mean BIS values are significantly lower in the patients with poor outcomes (CPC of 1 and 2) [48, 60–67]. A BIS cutoff-point in a range of 35–45 has shown an accuracy above 0.85 in prediction of the poor outcome [60, 61, 63, 65, 67]. More details about the results of these studies can be found in Table 2.

Table 2: Summary of the State-of-the-Art in employment of quantitative EEG measures (features) for prognostication of outcome in the cardiac arrest subjects treated with hypothermia

Feature group	**Features name**	**Feature's efficacy in cardiac arrest prognostication**
Conventional entropy-based measures	Spectrum entropy (SE)	- In a study of 20 rats, SE at 6-h post-ROSC was predictive of 96-h survival outcomes [33]
	Approximate entropy (ApEn)	- In a study of 46 comatose patients, the average ApEn was significantly higher in patients with good outcome (CPC 1–2) evaluated at 3-month post-CA[28]
	Multiscale entropy (MSE)	- In a study of 10 rats, alpha-rhythm MSE measured within 1–2.5-h post-CA was significantly different between the hypothermic and normothermic groups. Good recovery outcomes (NDS > 60) was always achieved if the ratio of alpha-rhythm MSE measured at 3-h post-CA to that of the baseline (before-CA) was above 0.85[26]
	Wavelet subband entropy (WSE)	- In a study of 30 comatose patients, Beta WSE measured between 24 and 48 h post-CA was significantly higher in the good outcome group (CPC of 1–2) evaluated within a 6-month follow-up period [21] - In a study of 11 comatose patients, 64–100 Hz WSE captured from the inferior frontal lobes were significantly higher in those survived [18]
	C0 Complexity	- In a study of 12 rats, C0 complexity measured as early as 4-h after the ROSC was significantly higher in hypothermic group than normothermic group. In fact, C0 complexity at 4-h correlated well with the 72-h NDS (correlation = 0.882)[44]
Burst suppression measures	Burst suppression ratio (BSR)	- In a study of 46 comatose patients, the average BSR was significantly lower in patients with good outcome (CPC 1–2) evaluated at 3-month post-CA [28] - In a study of 30 comatose patients, BSR during the first 48 h post-CA was significantly lower in the good outcome group (CPC of 1–2) evaluated within a 6-month follow-up period[21]

Feature group	Features name	Feature's efficacy in cardiac arrest prognostication
	Burst suppression frequency (BSF)	- In a study of 20 rats, BSF at 2-h post-ROSC was predictive of 96-h survival outcomes [33]
Information quantity measures	Information quantity (IQ)	- In a study of 28 rats, the 72-h NDS of the hypothermia group was significantly improved compared to the normothermia. The IQ also showed significantly different values between hypothermia and normothermia groups[25] - A study of 30 rodents showed that brain injury results in a reduction of IQ, and the average IQ of hypothermic rats was significantly higher than the normothermic rats for various injury levels [49] - In a study of 28 rats, IQ at 30-min post-CA had strong correlation of 0.735 with 72-h NDS scores[19]
	Subband information quantity (SIQ)	- In a study of 36 rats, SIQ values was significantly higher when hypothermia was administered immediately post-resuscitation and maintained for 6-h relative to when hypothermia started 1 h post-resuscitation and maintained 12 h[51] - In a study of 13 rats, SIQ showed a higher correlation (0.74) with 72-h NDS scores than IQ (0.65)[50] - In a study of 14 rats, both IQ and SIQ at as early as 1-h post-CA had high correlation (0.8) with 72-h NDS score [52] - In a study of 27 rats, the Gamma-band SIQ had the strongest correlation(between 0.52 and 0.78), while Delta-band SIQ had the lowest correlation to 72-h NDS score [53]
Combined measures	Cerebral Recovery Index (CRI) (combination of 5 features) Power, shannon entropy, alpha to delta ratio, regularity, coherence	- In a study of 109 comatose patients, CRI at 24-h post-CA classified the good outcome (CPC 1–2) versus poor outcome (CPC > 2)[54] - CRI < 0.29 predicted poor outcomes (sensitivity = 55%, specificity = 100%) - CRI > 0.69 predicted good outcomes (sensitivity = 25%, specificity = 100%)

Feature group	Features name	Feature's efficacy in cardiac arrest prognostication
	Enhanced Cerebral Recovery Index (ECRI) (combination of 9 features) Power, shannon entropy, alpha to delta ratio, regularity, coherence, tsalis entropy area, cepstrum coefficients, Maximum Phase Lag Index, binary low voltage measure	- In a study of 167 comatose patients, ECRI measured in 24-h post-CA increased the classification accuracy of good outcome (CPC 1–2) versus poor outcome classification by an average of 27%[10]
	Bispectral Index (BIS)	- In a study of 62 patients, BIS was significantly higher in the good outcome group. BIS at 24 h post-CA was the best predictive of CPC 1–2 outcome compared to the other time points; a BIS cut-point of 45 exhibited a sensitivity of 63% and a specificity of 86%, with a positive likelihood ratio of 4.67[61] - In a study of 97 patients, BIS was higher in patients with good outcome (37 [28–40] vs. 7 [3–15]). BIS < 22 predicted poor outcome with a likelihood ratio of 14.2 and accuracy of 0.91 [60] - In a study of 75 patients, BIS values were significantly higher in patients with good outcome (CPC 1–2). patients with S100b level above 0.03 mg/l and BIS below 5.5 had a 3.6-fold higher risk of poor neurological outcome [64] - In study of 75 patients, using BIS < 40 as threshold criteria, poor neurological outcome(CPC 3–5) was predicted with a specificity of 89.5% and a sensitivity of 85.7%[63] - In a study of 509 patients, those who awakened early had significantly higher BIS values after the first dose of neuromuscular blockade [62]

Feature group	Features name	Feature's efficacy in cardiac arrest prognostication
		- In a study of 171 patients, BISi < 10 suffered 82% neurological-cause and 91% overall mortality, BISi 10–20 suffered 35% neurological and 55% overall mortality, and BISi > 20 suffered 12% neurological and 36% overall mortality [48] - In a study of 75 patients, BIS was significantly higher in good outcome (CPC 1–2). Analysis of BIS recorded every 30 min provided an optimal prediction after 12.5 h, with an accuracy of 0.89 [65] - In a study of 46 patients, BIS values were significantly lower in those who died (4 versus 34) [65] - In a study of 103 patients, Low mean BIS value best predicted poor outcomes with CPC of 3 to 5 with an accuracy of 0.861[67]

3.4 Discussion and conclusion

Early and accurate assessment of brain recovery and neurological outcome after CA can substantially help with the optimal healthcare management of the CA patients, and minimizing related emotional and financial costs for their families. Over the last few decades, several prognostication markers of CA outcome have been developed using various modalities including clinical examination, biochemical markers, electrophysiological testing, and neuroimaging [9]. Clinical examination outcomes such as the absence of motor response to painful stimuli, presence of myoclonus status epilepticus, and lack of brainstem reflexes have been widely used for CA prognostication [17, 68]. Biochemical markers of cerebral injury such as increased levels of lactate and Neuron-Specific Enolase (NSE) have been employed to predict the CA outcome, as well [69,

70]. The loss of distinction between gray and white matter measured by computer tomography (CT) [71], or reduced glucose metabolism detected by position emission tomography (PET) are other potential prognostication markers of CA outcome [72].

Hypothermia is shown to be one of the most effective neuroprotective methods for improving the CA functional outcome in animal models of global ischemia [33, 73, 74] and human clinical trials [75, 76]. Moderate hypothermia is the process of reducing the body core temperature to a range of about 32–34 °C (90–93 °F), and maintaining it for 12–24 h, to ensure organ perfusion and oxygenation [77]. However, the use of sedative and paralytic agents affects sensitivity of the conventional CA prognostication markers and changes their optimal timing for the outcome prediction [7, 9, 11–15]. Hence, currently there is no universally accepted method for CA outcome prognostication of the patients treated with hypothermia [7].

EEG monitoring has been shown to be useful in early CA outcome prediction [78], but the subjective and time consuming visual EEG interpretation limits its applicability as the preferred prognostic method. Automatic EEG pattern recognition using quantitative measures of EEG can overcome these barriers [54]. Thus, over the last few years there has been a growing interest in development and study of quantitative EEG prognostication markers [42]. Given the applicability of EEG monitoring and the significance of hypothermia in the prognostication of the CA outcome, in this work, we reviewed the existing literature on the employment of the quantitative measures of EEG to predict the outcome of CA in the patients treated with hypothermia.

An injury to the brain system can adversely affect its complexity. Thus, the use of entropy (a measure of system's complexity) may assist in tracking the recovery status of the brain after CA. Given this premise, a majority of the developed CA prognostication markers are entropy-based. Spectrum entropy, approximate entropy, multiple Scale entropy, and Wavelet subband entropy

have all proved to be useful in CA outcome prediction for the subjects undergoing hypothermia [18, 21, 26, 28, 33]. In general, higher values of these entropy-based measures have been shown to be associated with better neurological outcomes. Among the features, multiple scale entropy and Wavelet subband entropy can provide a more comprehensive characterization of the signal's complexity, as they include more spatiotemporal information.

However, they require higher computational complexity which may be an issue for automatic real-time EEG analysis.

A clinically accepted marker of brain injury is burst suppression activity in EEG [57]. Few burst suppression features have been successfully employed for CA outcome prediction during hypothermia [21, 28, 33]. Lower burst suppression ratio and higher burst suppression frequency have been generally associated with better outcomes.

Information quantity-based measures have demonstrated better tracking capability for both frequency changes and dynamic amplitude changes relative to conventional entropybased measures [19, 49, 52, 53]. Brain injury results in a reduction of information quantity, and thus, higher values of information quantity are associated with better outcomes.

It is well-known that brain is a non-linear time-variant system, and EEG is a quasi-periodic and non-stationary signal. Thus, a single EEG feature may only provide limited information about the status of such a complicated system. On the other hand, combining EEG features may improve the accuracy of CA prognostication. The original cerebral recovery index and its enhanced version were developed based on this premise [10, 54]. Although these two indices have demonstrated some promising results in CA outcome prediction, their further enhancement in terms of prediction sensitivity is needed to be clinically acceptable. Currently, there are few commercially available products to extract the EEG features. For example, the entropy module of Datex-Ohmeda (GE

Healthcare, Helsinki, Finland) can be used to extract state entropy, relative entropy, and BSR. BIS monitors by ASPECT medical systems, MA, USA can also extract BSR and BIS values. These commercially available monitors are simple to use by clinicians. However, some degree of variability among different monitors/models and consequently the extracted feature values should be expected, especially because some of these products (e.g., BIS monitors) have undergone various software/hardware updates throughout the years.

In general, significantly lower BIS values have been associated with poor outcome (CPC of 1 and 2) in CA patients [48, 60–67], and a BIS cutoff-point in the range of 35–45 has shown an accuracy of above 0.85 in prediction of the poor outcome in patients treated with hypothermia [60, 61, 63, 65, 67].

One potential approach to design a highly accurate CA outcome classification system is to apply advanced machine learning algorithms (e.g., support vector machines, decision trees) to a large vector of various EEG features (including those measured by commercially available products). Recent advancements in data mining techniques have enabled the efficient handling of the inherent variability in the extracted features (such as those due to employment of different BIS monitors). Inclusion of quantitative features from other modalities (e.g., biochemical markers or neuroimaging) could further enhance the classification accuracy [9, 21, 64]. For example, in [21], Wennervirta et al. showed that the accuracy of CA outcome prediction can be considerably improved by combining a biochemical marker (protein 100B) and an EEG feature (wavelet subband entropy). However, their small cohort study prevented them from performing statistically reliable techniques such as cross-validation to validate their prediction accuracy on an independent dataset. In a larger study cohort (75 patients), Stammet et al. were able to enhance the accuracy of

CA outcome prediction by more than 5% (statistically significant) with combining the S100B and BIS information [64].

In general, the reliable implementation of machine learning approaches requires a large dataset of CA subjects with clear documentation of physiological and clinical data following CA. A potential solution to overcome this challenge is the conduct of multi-institution research collaborations where the multimodality data is consistently and uniformly collected and shared among researchers to facilitate the development of reliable methods to predict the CA outcome.

CHAPTER 4: STUDY DESIGN

4.1 Collection of the data

Patients who underwent therapeutic hypothermia after cardiac arrest must have met the criteria based on their neurological exam. In addition, Long Beach Memorial hospital hypothermia guidelines required the ED physician to contact the neurologist prior to induction of hypothermia for appropriate patient selection. The neurologic exam to start the protocol was prior to start of sedation after spontaneous return of circulation had occurred. The patients who were to be undergoing hypothermia protocol were required to be unresponsive, not following commands, or Glasgow Coma Scale (GCS) < 8.

Note: After a traumatic brain injury the level of patient's consciousness is described by a scoring system called Glasgow Coma Scale.

4.2 Patient's data

A retrospective study of the EEG data collected from 11 comatose adult patients (5 Males and 6 females, aged between 40 to 82 years old) was conducted. These patients were admitted from April to October 2011 to the ICU of the Long Beach Memorial Medical Center and treated with TH after the successful resuscitation from CA. Approvals of the study were obtained from the Institutional Review Boards of Long Beach Memorial Medical Center and California State University, Long Beach with the waiver of informed consent, because EEG was part of standard patient care.

The IV injection for the therapeutic hypothermia was started (2.9±1.4) hours following the patients' admission to the hospital. It took an average of (3.6±2.5) hours for the patients to get to the targeted temperature. The patients were kept at the hypothermia stage for an average of (24±0.1) hours. Then their body temperatures were adjusted back to the normal temperature through a rewarming process with an average time length of (16±1.7) hours. Out of the 11

comatose patients, 4 had survived. EEG signals of the patients were captured from the following 16 channels: FP1-FP2, F3-F4, C3-C4, P3-P4, O1- O2, F7-F8, T3-T4 and T5-T6.

4.3 Patient demographic

Baseline demographic variables, including gender, age and initial arrest rhythm, were comparable between survived and non-survived patients (Table 3).

Table 3: Patient demographic

Patient baseline characteristics	Survived patients (n=4)	non-survived patients (n=7)
Female gender, number (%)	100	2 (28.57)
Median age, years(range)	56.6 (40-77)	60 (57-82)
Initial CA rhythm ventricular fibrillation, number (%)	3 (75)	4 (57.14)

4.4 Study Limitations

The retrospective nature of study impose some limitations to the study. For example the distribution of the dataset in terms of number of patients with a specific survival outcome (or functional outcome) would affect our hypothesis testing results. In addition, the inter-subject variability that inherently exists with respect to the time interval from collapse to restoration of spontaneous circulation, or how hypothermia is managed (how long after the cardiac arrest the hypothermia was initiated and how long it has been maintained) would affect the result of the study. Another issue will be the availability and duration of continues EEG (cEEG) recording over the course of TH intervention. These are limiting factors that may affect the result of our study.

CHAPTER 5: DATA PROCESSING METHOD

5.1 Data processing steps

Our method of this study consists of four major steps:

A. EEG signal preprocessing;

B. Discrete wavelet transform;

C. Calculation of wavelet sub-band entropy; and

D. Statistical Analysis.

Figure 6 illustrates a block diagram of various steps of the implemented method. In the following sections, each step is explained in details.

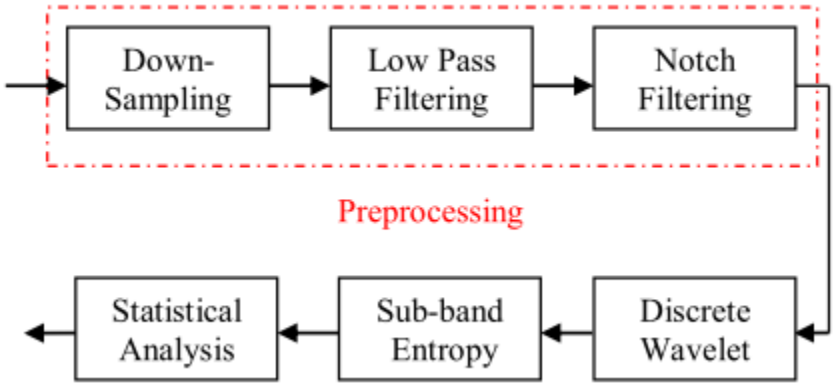

Figure 6: A block diagram of the implemented EEG processing method

5.2 Preprocessing

EEG signal were captured by standard 10-20 positioning system at Long Beach Memorial Hospital. For each patient different length of signals were available during the hypothermia and normothermia phases. The sampling rates were vary between patients and recording episodes (500, 1000. 1024. 2040 Hz). After a careful review of signals we found a high level of noise to signal

ratio on earlobes and midline channels (A1, A2, Fz, Cz and Pz).Therefore it was decided to not considering these signals in the signal processing phase due to a high level of the noise (Figure 7 and Figure 8). EEG signals that were captured from the following 16 channels were considered in the signal processing phase: FP1-FP2, F3-F4, C3-C4, P3-P4, O1- O2, F7-F8, T3-T4 and T5-T6.

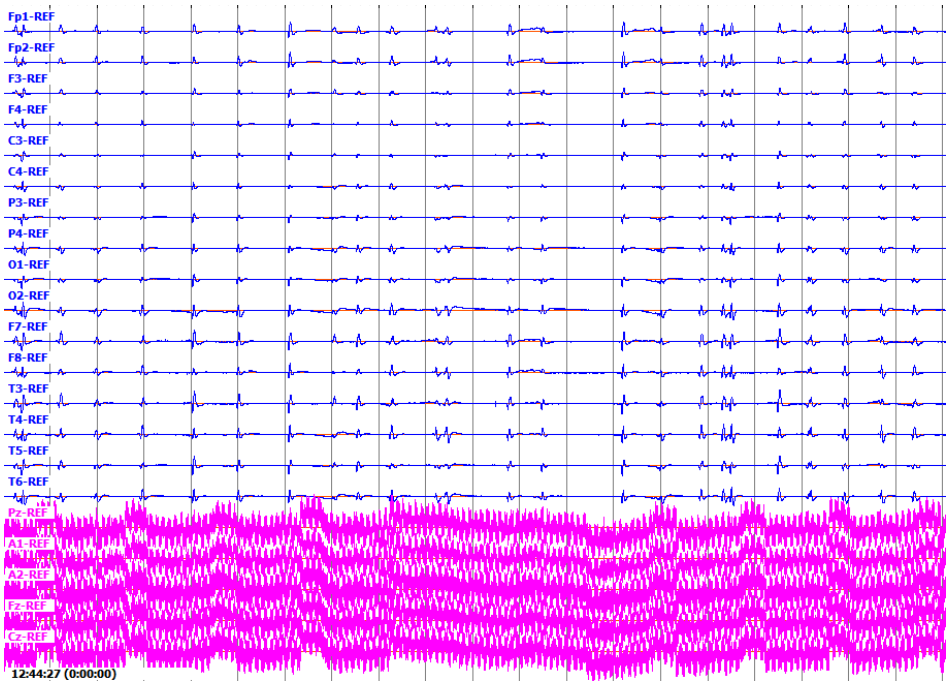

Figure 7: All EEG channels

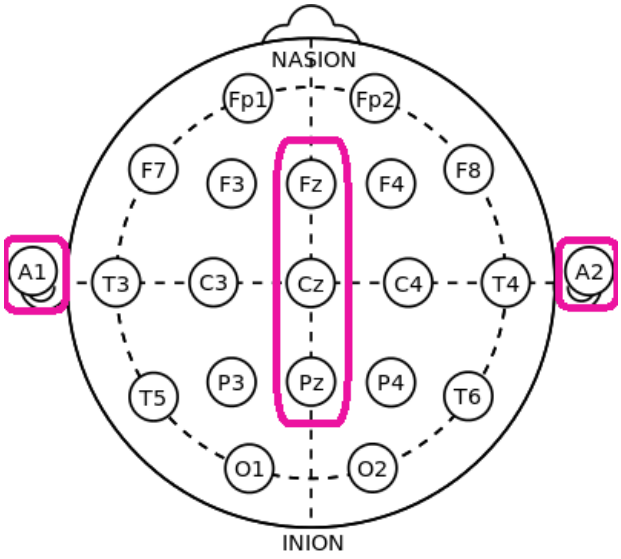

Figure 8: Location of signals with high rate of noise to signal value

Cz ,Pz and Fz are ground or common reference points for all EEG electrodes
A1 - A2 are used for contralateral referencing of all EEG electrodes

The EEG signal of each channel was first down sampled to 256 Hz to reduce the computational complexity. Given that the main frequencies of the human EEG waves are between 0 and 100 Hz, a linear phase Butterworth band-pass filter with passband of 0.15-100 Hz was applied to remove low and high frequency noise and artifacts [84]. Then a linear phase Butterworth notch filter at 60 Hz was applied to remove the power-line interferences.

Note: The magnitude of the frequency response for Butterworth filters calculated as follow:

$$|H(j\omega)|^2 = \frac{G_0^2}{1+(\frac{j\omega}{\omega_c})^{2n}}$$

Where n is the order of filter, ω_c is the cutoff frequency and G_0 is the gain at zero frequency.

5.3 Discrete Wavelet Transform

Wavelet transform has proved to be a useful tool for denoising, delineation and compression of signals. In contrast to Fourier transform, wavelet transform allows for the analysis of transients, non-stationary and aperiodic signals (such as spikes and bursts) by highlighting the subtle changes in signal morphology over various scales of interest. Discrete wavelet transform has few additional advantages (comparing to continuous wavelet transform) including less redundancy and lower computational complexity.

Given the sampling frequency of 256 Hz, using a 6-level discrete wavelet transform, one can decompose the EEG signal into frequency sub-bands that represent standard clinical bands of interest: Delta (< 4 Hz), Theta (4-8 Hz), Alpha (8-16 Hz), Beta (16-32 Hz), Gamma (32-64 Hz), and high frequency oscillation (> 64 Hz).

A Daubechies3 mother wavelet was employed to implement discrete wavelet transform. This mother wavelet can help in capturing spiky EEG waveforms due to its shape (Figure 9).

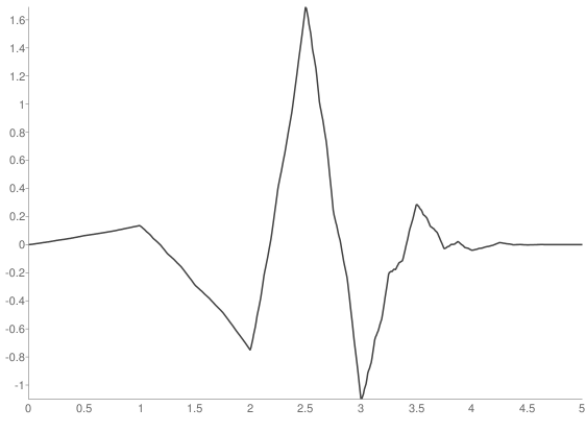

Figure 9: Daubechies3 wavelet function

5.4 Wavelet Sub-band Entropy

In this study, wavelet sub-band entropy [83] was employed as a quantified measure of EEG to predict the death and survival outcomes.

Let us assume that C_m^l is m^{th} wavelet coefficient at level l, where $l = 1,2,...,6$ and $m = 1,2,...,M$. Note M is the length of the coefficient vector (in samples) at each level of the decomposition. Each C_m^l was first squared and normalized as

$$\mathbf{C}_m^l = \frac{(C_m^l)^2}{\sum_{m=1}^{M}(C_m^l)^2}. \qquad (20)$$

Then the wavelet sub-band entropy (E^l) was obtained by calculating Shannon entropy of the normalized coefficients at each level:

$$E^l = \frac{-\sum_{m=1}^{M}\mathbf{C}_m^l \times \log(\mathbf{C}_m^l)}{\log M}. \qquad (21)$$

Filter tree algorithm for discrete wavelet transform (DWT) is shown in Figure 10:

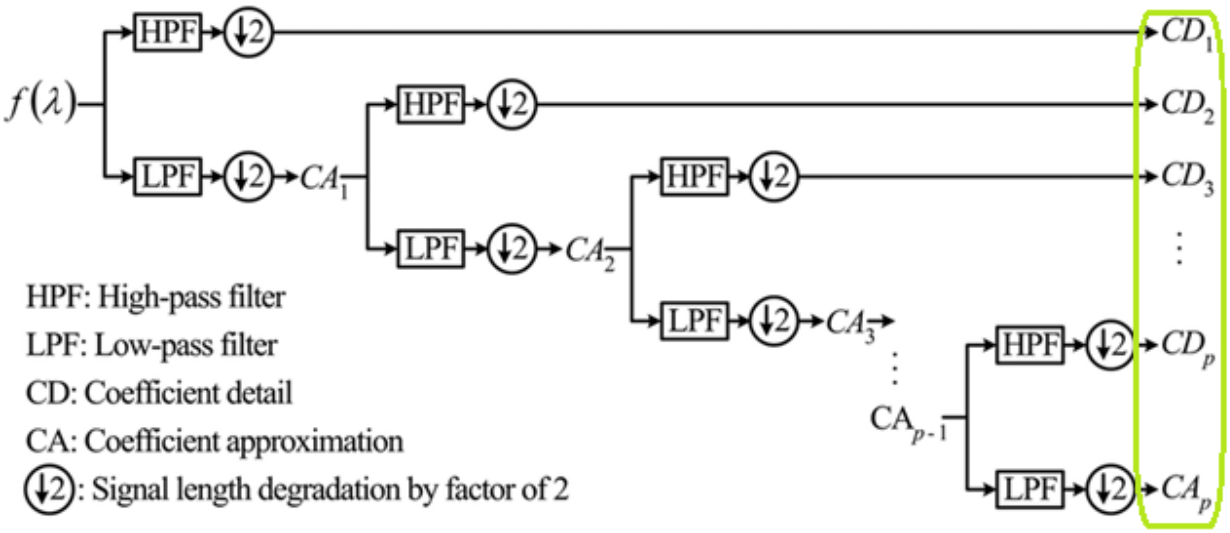

Figure 10: filter tree algorithm for discrete wavelet transform (DWT) picture reference [105]

5.5 ANOVA Mathematical Details

ANOVA tests for the difference in the group by splitting the Total Variability into two components:

- variation between groups
- variation within group

There are three assumptions for ANOVA test that should be satisfied to get the completely reliable results from analysis:

- independence of cases
- Normal distribution of the residuals
- Equality of variance

Usually failing to have the normal distribution of the measurement variables may result to increase the false positive (FP) rate in tests that have normality assumption for their under test data. Based on a simulation study to check the effect of non-normality distribution on ANOVA test, it was

concluded that the FP rate was not affected significantly by violating from this assumption [107, 108, 109].

Variation between groups is defined as group means variation from the overall mean:

$$SSR = \sum_{i=1}^{k} n_i(\bar{x_i} - \bar{x}) \qquad (22)$$

Where $\bar{x_i}$ is the sample mean value, n_i is the sample size of i^{th}group and $\bar{x}$ is the overall mean. $i = 1,2, \dots, k$.

Variation within group is defined as variation of observations in each group from their group mean estimates.

$$SSE = \sum_{i=1}^{k} \sum_{j=1}^{n_i} (x_{ij} - \bar{x_i})^2 \qquad (23)$$

Where the x_{ij} is thej^{th}response sampled from the i^{th} group.

ANOVA partitions the sum of squares total (SST) into sum of squares due to between-groups effect (SSR) and sum of squared errors (SSE).

$$SST = SSR + SSE = \sum_{i=1}^{k} \sum_{j=1}^{n_i} (x_{ij} - \bar{x})^2 \qquad (24)$$

ANOVA calculates the ratio of the variation between groups (*SSR*) to the variation within groups (*SSE*). If this ratio is significantly high, then it can be concluded that the group means are significantly different from each other.

The test statistics with F-distribution (with (*k – 1, N – k*) degrees of freedom) is defined as follow:

$$F\ Statistic = \frac{SSR/(K-1)}{SSE/(N-k)} = \frac{MSR}{MSE} \sim F_{k-1,N-k} \qquad (25)$$

where *MSR* is called the mean squared treatment, *MSE* is the mean squared error, k is the number of groups, and N is the total number of observations.

If the *p-value* for the *F-statistic* is smaller than 0.05 (or 0.01), then the test rejects the null hypothesis. In ANOVA the null hypothesis is that all group means are equal. Small P-value means that at least one of the group means is different from the others [106].

5.6 Statistical analysis

A moving window of length T with 50% overlapping was applied to the recorded EEG signal of each channel and the wavelet sub-band entropies were calculated for each window. A one-way analysis of variance (ANOVA) test was employed to determine whether the calculated entropies are significantly different between those subjects who survived and those who died. The ANOVA test was repeated for all the 6 levels and all the 16 EEG channels. Our hypothesis was that the EEG signals of the patients who survived would demonstrate more complexity and consequently higher values of wavelet sub-band entropies.

CHAPTER 6: SWE RESULTS

6.1 Results

Various window lengths were used (including T of 10 seconds, 30 seconds and 60 seconds) to test our hypothesis. Interestingly, the results were similar regardless of the window length.

The normality distribution of the data under test were analyzed to make sure that the data distribution satisfies the ANOVA assumptions. A sample graph of the normality results is shown in Figure 11:

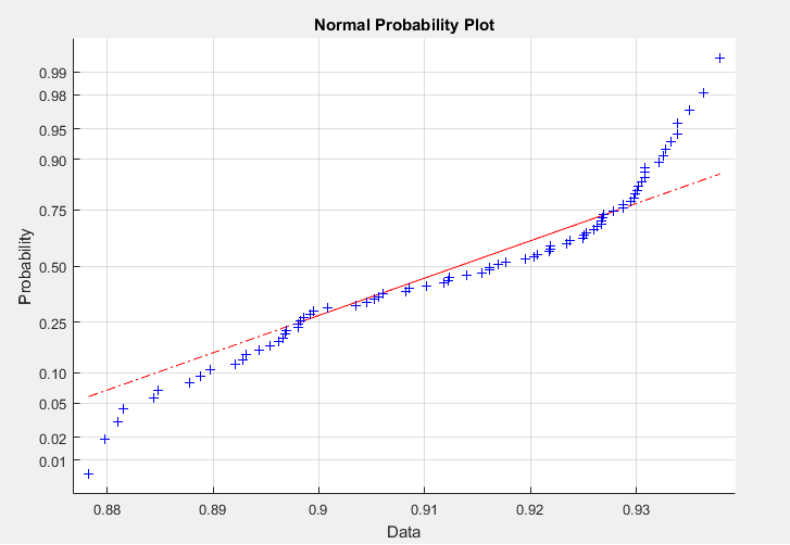

Figure 11: Check the normality of data for ANOVA (Sample plot)

Our data analysis revealed that out of all the wavelet sub-band entropies calculated for various frequency bands (representing standard clinical bands of interest) and over 16 different EEG channels collected during hypothermia, only the wavelet sub-band entropies of high frequency oscillations (HFO in this study: 64-100 Hz) that are captured from the inferior frontal lobes (F7 and F8) are associated with the CA outcomes.

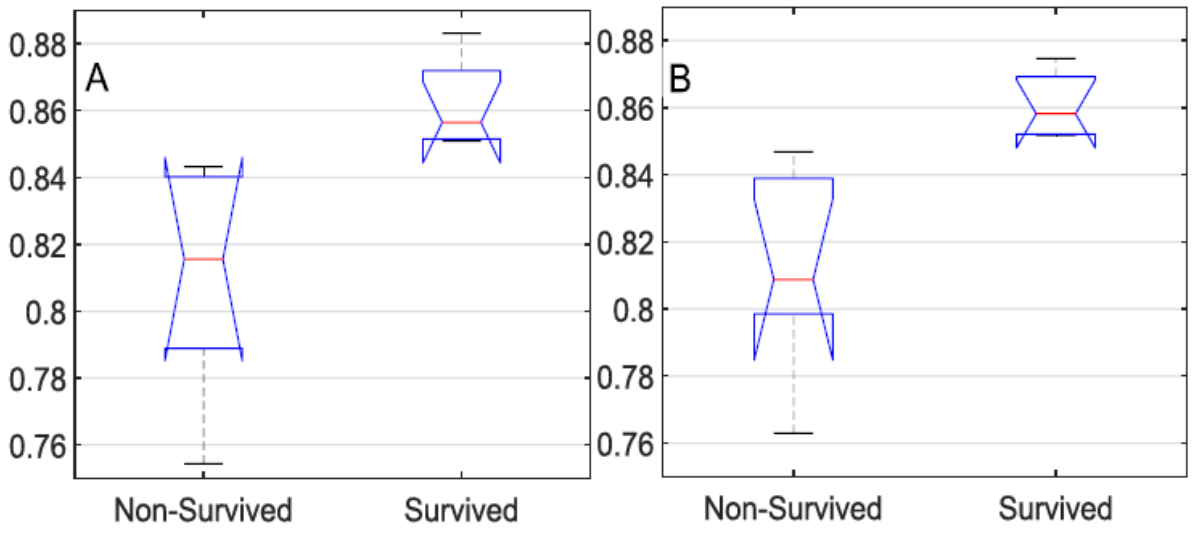

Figure 12: Boxplots of high frequency oscillation sub-band (64-100 Hz) wavelet entropies over inferior frontal: A) F7 EEG channel; B) F8 EEG channel.

Figure 12 illustrates the box plots of the HFO sub-band entropies calculated from the EEG of the inferior frontal lobes (F7 and F8) for the survived and non-survived outcomes when T=1 minute. It can be noted that the mean HFO sub-band entropies of both F7 and F8 EEG channels are significantly higher in the patients who survived than those who died. The p-values for F7 and F8 channels were 0.01 and 0.02, respectively.

Figure 13A displays a one-minute sample of EEG signal captured from the inferior frontal lobes of one of the patients who survived, while Figure 13B illustrates a sample of EEG signal from a patient who died. The EEG signal of the survived patient displays more complexity. This is consistent with our hypothesis that the patients who survive would have more complexity and consequently higher entropy values of EEG signals. Figure 14 shows the location of F7 and F8 channels on 10-20 system for electrode layouts.

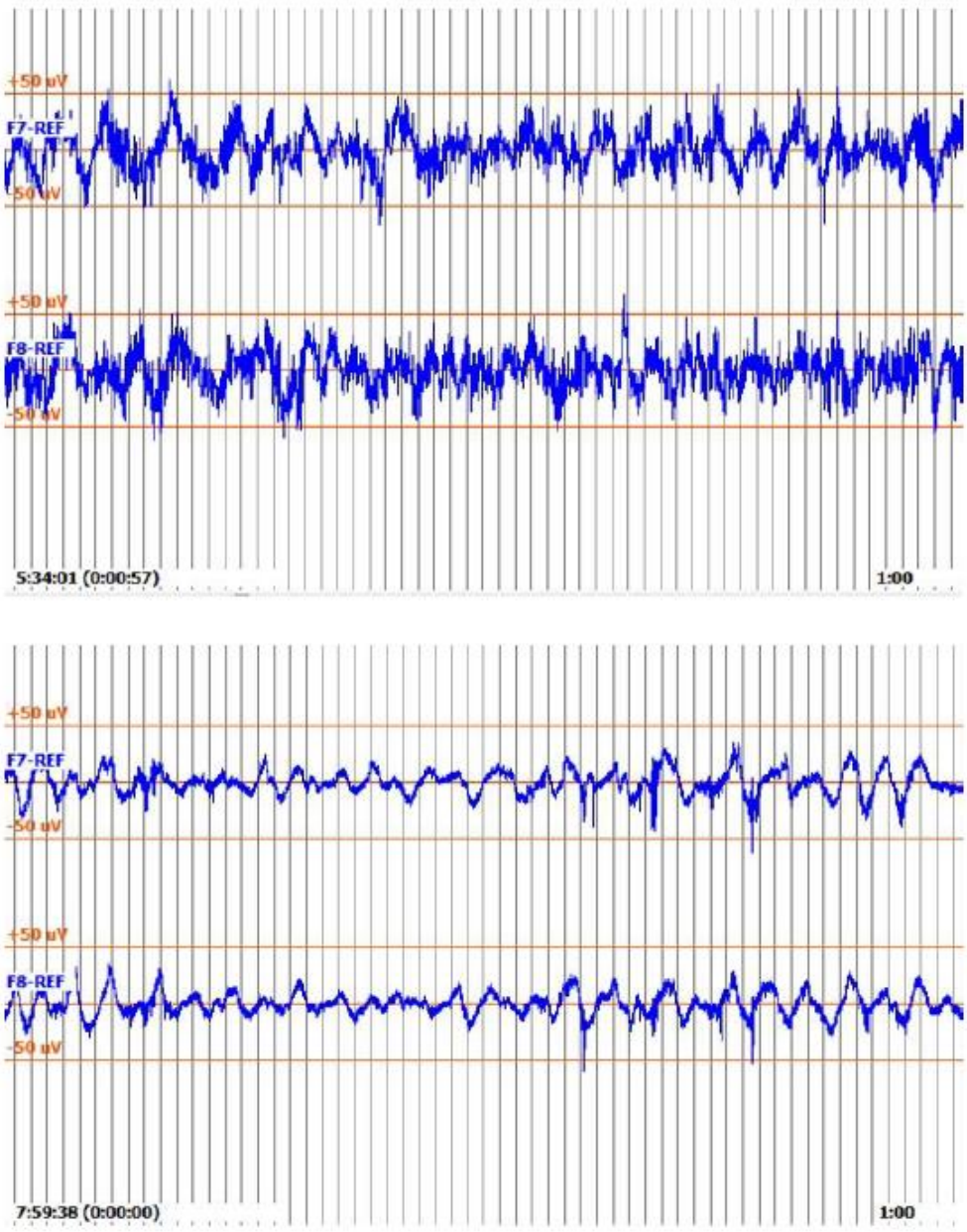

Figure 13: One-minute EEG signal captured from inferior frontal lobes (F7-F8) of A) a survived patient; B) a non-survived patient.

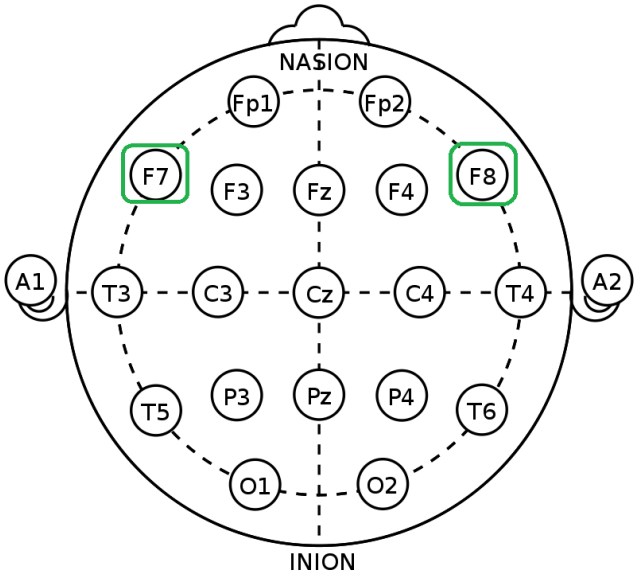

Figure 14: Location of F7 and F8 channels based on the 10-20 standard layout of EEG electrodes

Same analysis were done on the normothermia signals. ANOVA results revealed no significant differences between channels and frequencies during the normothermia phase in Survived and non_survived patients (Figure 15). The P_value was 0.6312.

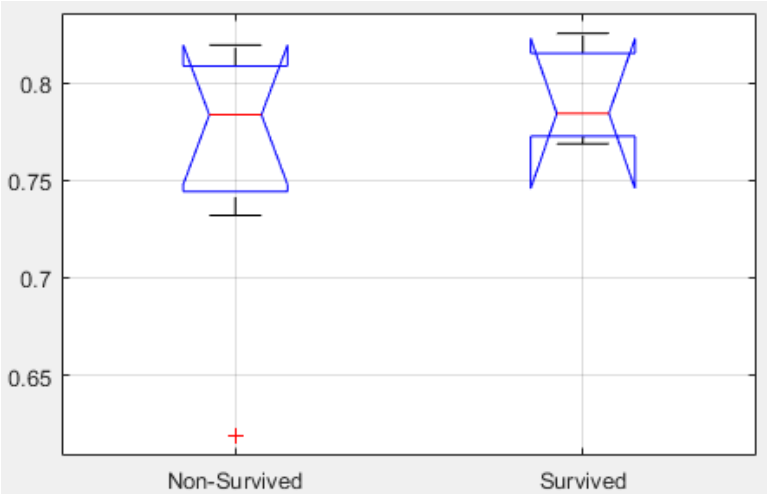

Figure 15: Boxplots of high frequency oscillation sub-band (64-100 Hz) wavelet entropies over inferior frontal during Normo-thermia

Figure 16 displays a one-minute sample of EEG signal captured from the inferior frontal lobes of one of the patients who survived during Hypothermia (a) and Normothermia(b), while Figure 16 illustrates a sample of EEG signal from a patient who died during Hypothermia (c) and Normothermia(d).

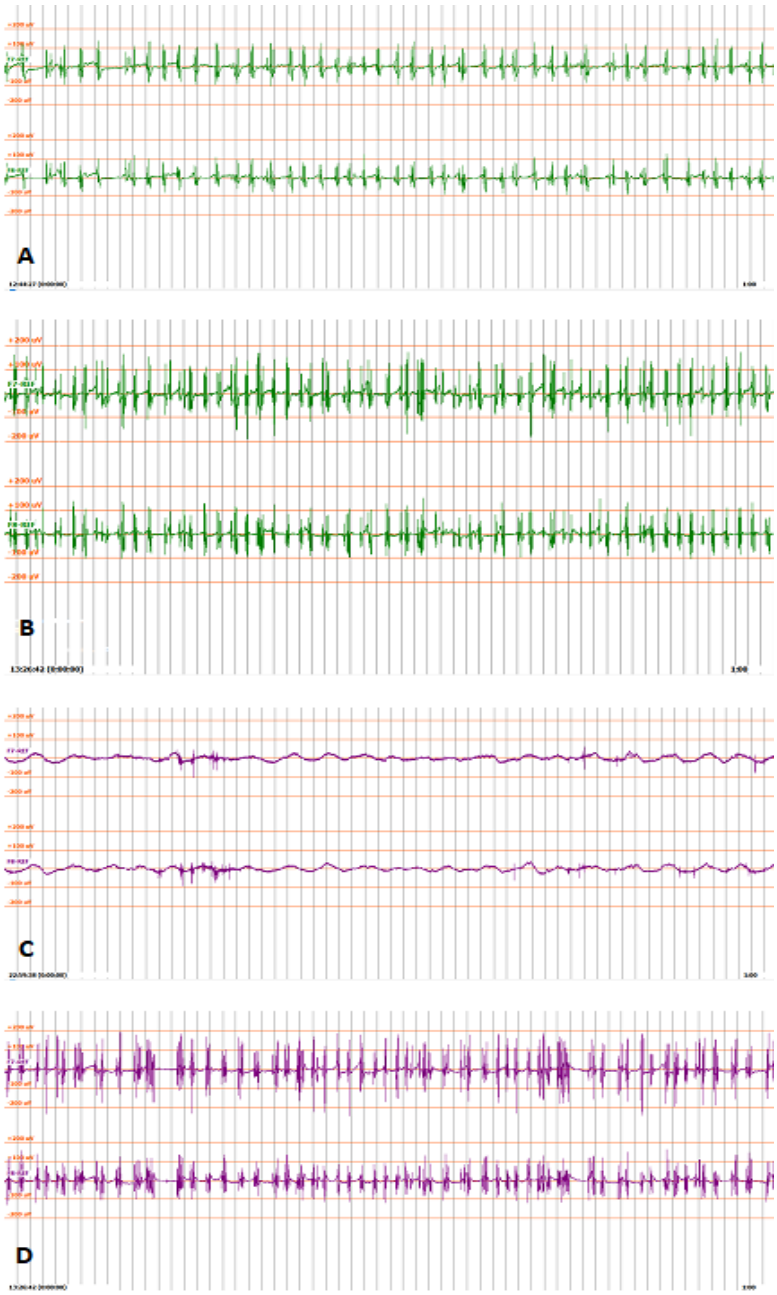

Figure 16: Comparison between Hypothermia and Normothermia signals in Survived and Non-survived patients

6.2 Discussion and Conclusion

The visual interpretation of EEG patterns, e.g., background and reactivity analysis, provides important information about the CA outcome, but is time-consuming and subjective. Automated EEG analysis may help in quantification of the brain damage following CA and the prognostication of the outcome [85]. Recently, several animal studies have successfully investigated the possibility of using quantitative measures of EEG during hypothermia, e.g., information quantity (IQ) and sub-band information quantity (SIQ), to predict the CA functional recovery outcome[79, 80-82]. However, to the best of our knowledge, only few human studies have employed quantitative measures of EEG, e.g., burst-suppression ratio and state entropy, to predict the outcome of CA patients treated with hypothermia [85, 86].

In the present study, we sought to examine whether any of the EEG wavelet sub-band entropies calculated over various frequency bands of clinical interest and for 16 different EEG channels can be used to distinguish the survival versus death outcome in CA patients undergoing hypothermia. Our results demonstrated that the high frequency oscillations (HFO: 64-100 Hz) of inferior frontal lobes during hypothermia were more complex in the people who survived. It is known that the frontal lobe is considered as “the most human structure” of the brain, because frontal lobe is larger and more developed in humans than in any other organism. F7 EEG electrode is located near the center of rational activities (related to verbal and cognitive activities), while F8 is close to the sources of emotional responses (endogenous). Therefore, our results indicate that, during hypothermia, high frequency oscillations that are captured from inferior frontal (related to the cognitive and emotional responses) demonstrate more complex patterns in the patients who survive. These results are consistent with those of recent studies showing that the presence of HFOs after CA may indicate good functional recovery [87, 88].

Hence, recovery of high frequency brain activities should be a main target to recover neurological functionality post-CA. One of the limitations of the present work was the small sample size which could not be adjusted due to retrospective nature of the study. Our future work will involve a prospective study of a larger dataset of CA patients undergoing hypothermia to further verify the reliability of the developed prognostic marker of CA. A dataset with more number of subjects would also allow us to enhance the validity of the statistical analysis by considering other variables (e.g. age) that could play a significant role in the CA outcome.

In conclusion, this study showed that wavelet sub-band entropy of EEG high frequency oscillations captured from inferior frontal lobes can be successfully employed to prognosticate CA outcome for patients undergoing hypothermia. The result of this study can improve the quality of care for CA patients by early prediction of the outcome.

CHAPTER 7: WAVELET COEFICIENTS SPECTRAL ENTROPY (WCSE)

7.1 Wavelet Coefficients Spectral Entropy (WCSE)

As the next step of this study, we decided to do the same analysis with different quantitative measures.

Kumar et al. [110] used a classification method to automatically detect the epileptic seizures. They selected two main entropy features, Wavelet Entropy and Spectral Entropy, to test and train the recurrent neural network classifier. They achieved high classification accuracy results in their studies. They also concluded that Wavelet entropy feature provides more accurate results in compare to spectral entropy feature [110]. This study highlighted the ability of wavelet entropy and spectral entropy quantities to detect EEG abnormalities among of all other different quantitative EEG features that can be developed.

Mirzaei et al [88], calculated the spectral entropy of wavelet coefficients of EEG signal to detect the epileptic seizures. They found significant differences between SE values in Ictal and healthy subjects.

Chen et al. [33], applied the Spectral Entropy method on EEG signals of rats to evaluate the CA outcome. They concluded that the spectral entropy (SE) values was higher in the hypothermic rats. Wennervirta et al., in a study of 30 comatose patients concluded that the spectral entropy demonstrated significantly higher values in CA patients with good cerebral performance category (CPC) outcomes.

Given the success of wavelet transform for analyzing the components of a non-stationary signals in different frequency levels, and spectral entropy as a successful feature to distinguish EEG abnormalities, we combined these tools to create a better marker in order to distinguish between survived and un-survived cases.

As it was discussed before (see section 3.3.1.1), in most of the previous studies the spectral entropy were measured by commercially available products with limited frequency bands of 0.8–32 Hz (state entropy) and 0.8–47 Hz (response entropy). Because of various software/hardware updates throughout the years over these tools there are some variability exists between their extracted spectral entropy features.

Therefore, as our next step of study we developed a new EEG quantitative measure, Wavelet Coefficients Spectral Entropy (WCSE). We calculated the spectral entropy of each sets of Wavelet Sub-band Coefficients. So instead of having the SE value only for limited range of frequencies, we can analyze the SE value for all clinical sub-band frequencies.

Then we compared the value of wavelet coefficient spectral entropy between survived and un-survived patients. Our goal was to find significant differences between the WCSE value of Survived and un-survived CA patients. We expected to have higher WCSE value in survived patients.

7.2 WCSE Method

In this step of our study, we followed the same preprocessing of the data that was introduced in Sub-band wavelet entropy section.

In order to retrieve the useful signals Butterworth band pass filter has been applied and Interference noise has been filtered by a notch filter. Figure 17 illustrates the overall specification of the bandpass and notch filters. Then after applying the 6-level discrete db3 wavelet transform, the spectral entropy of each set of wavelet coefficients were calculated.

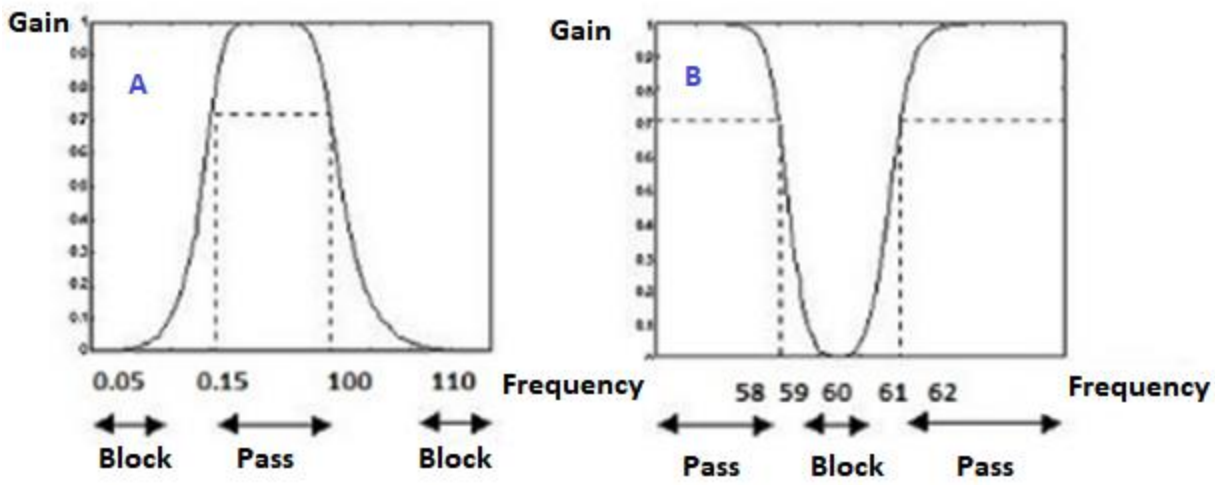

Figure 17: Butterworth filters specification, A) Bandpass, B) Notch

The wavelet coefficient spectral entropy (WCSE) of the EEG signal is calculated as the Shannon entropy of the normalized energy distribution of the signal within certain frequency sub-bands of interest.

To calculate the WCSE value, the same method that was described by Mirzaei et al [88] and Liu et al. [110] were applied:

A moving window of length T (T=60 sec) with 50% overlapping was applied to the recorded EEG of each channel and for each level of coefficients in each window, the normalized energy distribution calculated as follow:

$$P_i = \frac{E_i}{\sum_{i=1}^{N} E_i} \qquad (26)$$

where *Ei* is the energy of the coefficients'signal within *i*th subband calculated from power spectral analysis of the EEG signal.

Then the Shannon entropy of the normalized energy distribution calculated:

$$SSE = \frac{-\sum_i^N p_i \log_2 p_i}{\log N} \qquad (27)$$

N is the length of coefficient vector at each level of decomposition.

Then the ANOVA test applied to determine if the calculated WCSE is significantly different between survived and non-survived subjects. We hypothesis that WCSE value for survived patients demonstrates higher value in compare with non-survived patients.

The ANOVA test was repeated for all 6 levels and 16 EEG channels.

7.3 WCSE Results

The data analysis reveals that out of all Wavelet Coefficients Spectral Entropies (WCSE) calculated for all standard clinical frequency bands during the hypothermia and over 16 different EEG channels only the WCSE of Theta band frequencies (4-8 Hz) that are captured from the C3 (left-central lobe) and F3 (Middle-left Frontal lobe) channels are associated with CA outcomes (Figure 18).

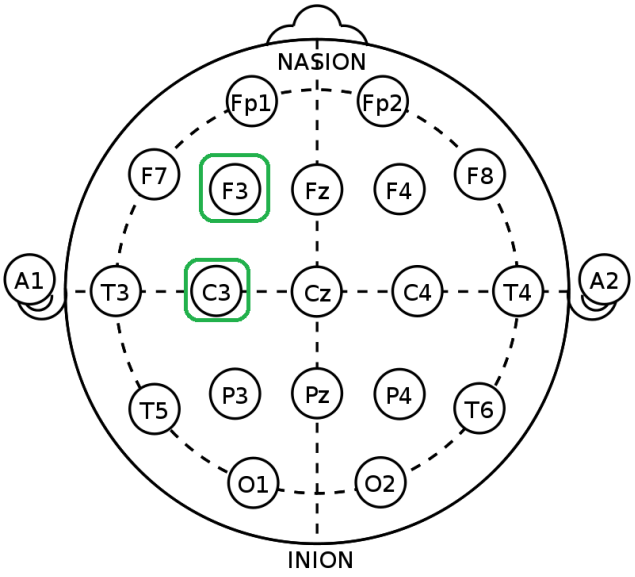

Figure 18: Location of C3 and C5 channels based on the 10-20 standard layout of EEG electrodes

The box plot of the theta band wavelet coefficients spectral entropies calculated from the central and middle frontal lobes for the survived and non-survived patients illustrated in Figure 19.

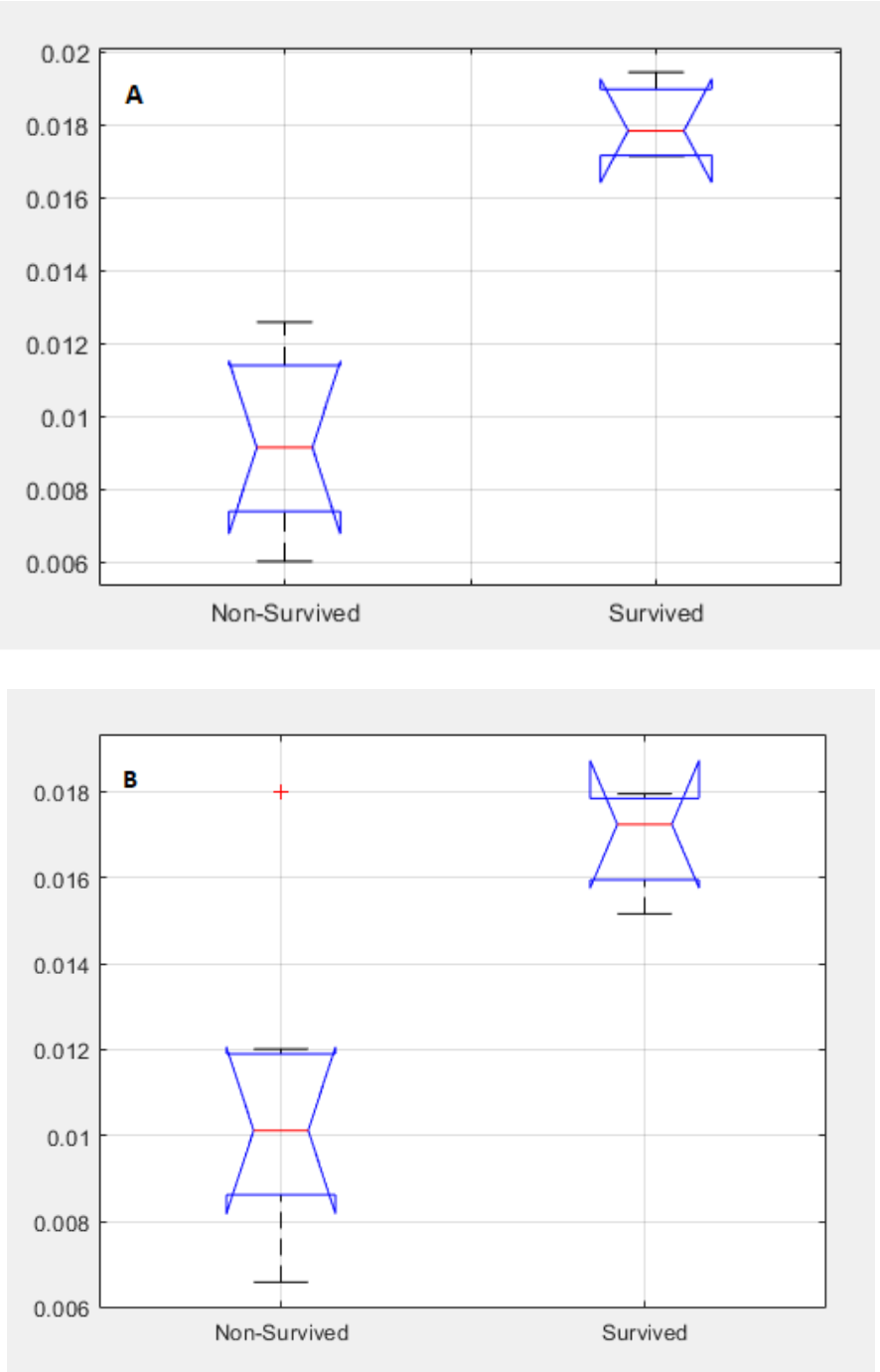

Figure 19: Boxplot of theta band frequencies (4-8 Hz) wavelet coefficients spectral entropies over C3 and F3 channels: A) F3 EEG channel, B) C3 EEG Channel

The mean of theta band wavelet coefficients spectral entropies for both C3 and F3 channels are significantly higher in survived patients in compare with un-survived patients with the p-value of 0.04 and 0.02, respectively. One-minute sample EEG captured form C3 and F3 channels for survived and non-survived are displayed in Figure 20.

It is clearly illustrated that the survived patients EEG signal is more complex. These results are consistent with the hypothesis that the spectral entropy (SE) values was higher in the survived patients due to more complexity of EEG signals.

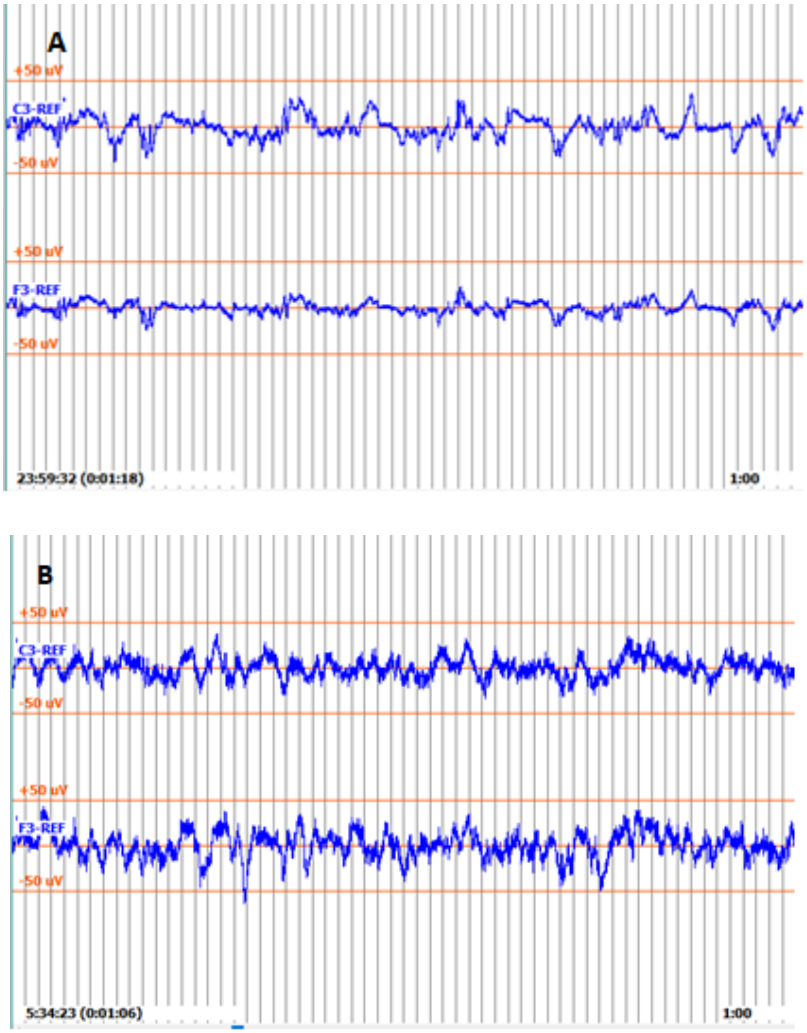

Figure 20: one minute EEG signal captured from C3 and F3 channels: A) Non-survived patient, B) Survived patient

7.4 Discussion and Conclusion

Our goal in this phase of study was to examine the wavelet coefficients spectral entropies (WCSE) as a quantitative marker of the CA patients' outcome. Our results demonstrated that the theta frequencies of left central lobe (which is related to sensory and motor functions) and middle-left frontal lobe (related to motor planning and actions) during hypothermia were more complex in the people who survived.

Theta band waves are low-frequencies components of EEG signal, typically ranged from 4 to 8 Hz. Theta rhythms are commonly encountered in the fronto-central regions in healthy brains. Theta rhythm is considered abnormal if is observed in a different location [113, 114]. Theta band frequencies are usually related to drowsiness or heightened emotional states [112].

Grunwald et al. found that that fronto-central theta power of the EEG correlates with the load of working memory independent of stimulus modality. They showed in their study that the theta waves powers in the EEG of human subjects increases during recall of haptic information [114].

In summary, our results indicate that, during hypothermia, EEG theta frequencies that are captured from fronto-central regions (C3-F3) demonstrate more complex patterns in the patients who survive. These results are consistent with those of studies showing the correlation of higher values of SE and good functional outcome [33] and the presence of fronto-central theta rhythms in normal and healthy brain [113].

7.5 Discussion on Left and Right Brain Hemisphere Differences

Functions and characteristics of each hemisphere are well established. The left hemisphere controls the right side of the body and responsible for analytical thinking and logical tasks while most of

the visualization and emotions, as well as the left side of the body, are controlled by the right hemisphere.

Henda et al. studied the functional outcome and mortality between left- and right-hemisphere ischemic strokes. They concluded that the left-hemispheric ischemic strokes appear to be more frequent and often have a worse outcome (higher risk of mortality) than their right-hemispheric counterparts [115].

In our study, we developed two quantitative EEG markers, Sub-band Wavelet entropy (SWE) and Wavelet Coefficients Spectral Entropy (WCSE), to predict the outcome of cardiac arrest patients treated with hypothermia.

Our results revealed that the brain high frequency oscillations (Gamma Band: 64-100 HZ) SWE is higher in inferior Frontal lobe and theta band (4-8 Hz) WCSE is higher in left side fronto-central lobes of survived patients. Figure 21 illustrates the location of all EEG channels that were associated with CA outcome.

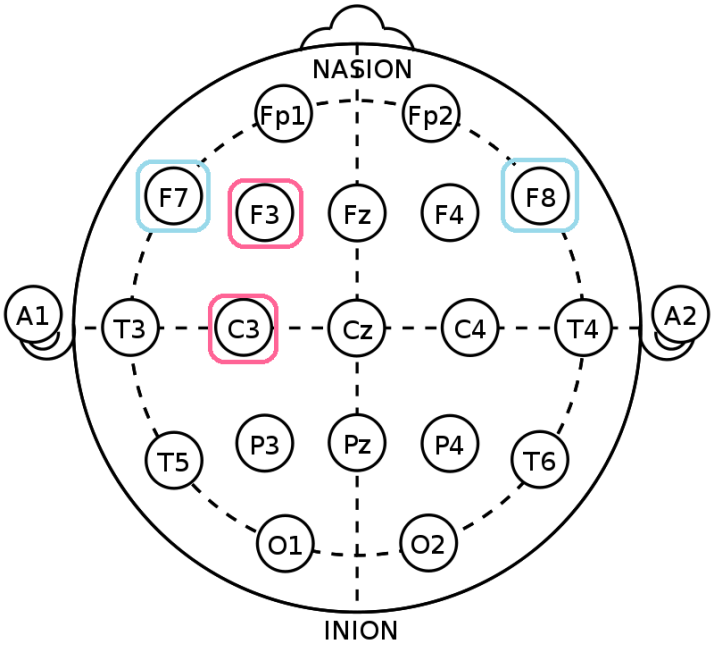

Figure 21: EEG channels associated with good outcomes, Pink: WCSE results, Blue: SWE results

As it is shown in the Figure 21, three out of four of these distinguished channels in survived patients are located in the left hemisphere which is consistent with the study showing that the less damages on left hemispheric may increase the chance of good outcome in ischemic strokes patients [115]. Also, Frontal lobe (Middle and Inferior) which is considered as the "most human structure" of the brain shows more complexity in both studies in survived patients.

Therefore, recovery of the Gamma and Theta frequency activities on left-hemisphere and/or Frontal lobe can be main target for post cardiac arrest recovery.

Given all the limiting and confounding factors that this retrospective study has, we still believe that performing such study would be substantial as it employs a new approach (automatically quantified cEEG measure, i.e. entropy) to predict patient outcome after cardiac arrest.

Furthermore, the experience that we learn from this study, can guide us to design a prospective study aiming at the same objective and addressing all the limiting and confounding factors to guarantee the future success of the study.

CHAPTER 8: SINGULAR-VALUE DECOMPOSITION (SVD)

8.1 Background: Question that was raised during the Qualification exam

"Assume you do not know which patient survived and which did not, assume that you collected all the original signals obtained from all sensors attached to the frontal zone from all the patients (the total number of signals is equal to the total number of the sensors in frontal zone multiplied by the total number of the patients) and you first use SVD to reduce the number of dimensions and after that you use say K-means to split the signals into two clusters. Will all signals form the survived patients be in cluster one and all signals from the patients who did not survive in the cluster two, if you use say just only 3 principal components for SVD? "

8.2 Introduction to Singular-Value Decomposition (SVD)

The Singular-Value Decomposition (SVD) is a matrix decomposition method for reducing a matrix to its fundamental elements in order to make certain subsequent matrix calculations simpler. Because SVD can be calculated for all matrices, it can be used as a stable method for data and dimension reduction purposes [116].

SVD for a rectangular *m-by-n* matrix A is calculated as:

$$A = U.\Sigma.V^H \qquad (28)$$

Where U is a *m-by-m* matrix, Σ is a *m-by-n* diagonal matrix and V is a Hermitian *n-by-n* matrix. The values in the Sigma diagonal matrix are the singular values of the matrix A. The columns of the U matrix are called the left-singular vectors of A are in columns of the U matrix and the right-singular vectors of A are the columns of the V matrix [116].

When we have a matrix of data with larger number of features than observations, by using SVD method we can find the most relevant features. SVD reduces the dimension of the data matrix and this lower rank matrix can be used as a good approximation of the original data.

The approximation matrix can be calculated by applying the SVD on the original data and finding the top K largest singular values from Σ matrix and their corresponding values from V^H matrix [116].

8.3 K-mean clustering

K-mean clustering is a method that partition the observations (n data points) into desired K clusters. Each cluster is defined by its centroid point. The algorithm go through following steps [117]:

- Choose k initial cluster centers (centroid)
- Compute point-to-cluster-centroid distances of all observations to each centroid
- Assign each observation to the cluster with the closest centroid.
- Compute the average of the observations in each cluster to obtain k new centroid locations.
- Repeat steps until cluster assignments do not change

8.4 SVD Analysis and K-mean clustering – Phase I

Based on the prior knowledge from Wavelet Sub-band Entropy analysis, that the Frontal lobe's electrodes have significant differences in survived and non-survived patients, we applied the singular-value decomposition (SVD) and K-mean clustering analysis over the frontal lobe's electrodes (F7 and F8).

We hypothesized that the non-survived data points should cluster together and the survived data points should cluster together.

Here are the steps of this analysis:

- Extracted filtered data from F7 (and F8) channels during hypothermia for all patients
- Down-sampled the data to avoid getting overloaded error
- Applied SVD Matlab built-in function to define eigenvalues (calculate the Covariance of eigenvalues)
- Plotted the eigenvalues (descending order)
- Calculated the projection matrix of all patients' channel 7 (and channel 8) data (both 2 dimensions and 6 dimensions (See Figure 22) calculated for comparison purposes (matrices 11x2 and 11x6))
- Applied 2 groups' k-means clustering.
- Calculated the Accuracy and Sensitivity (true positive rate) of the results

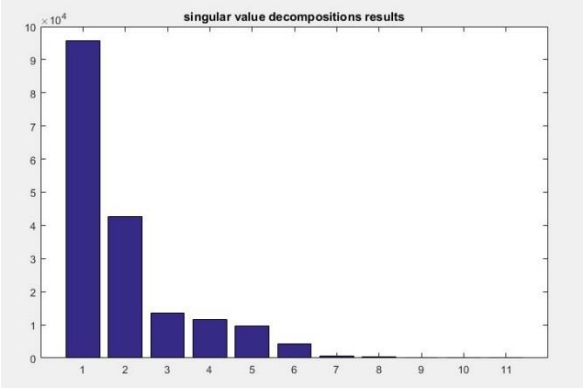

Figure 22: Sorted eigenvalues

8.5 SVD Results- Phase I

The Survived and non-survived data points were clustered together with the accuracy of 72% and Sensitivity of 60% (Figure 23).

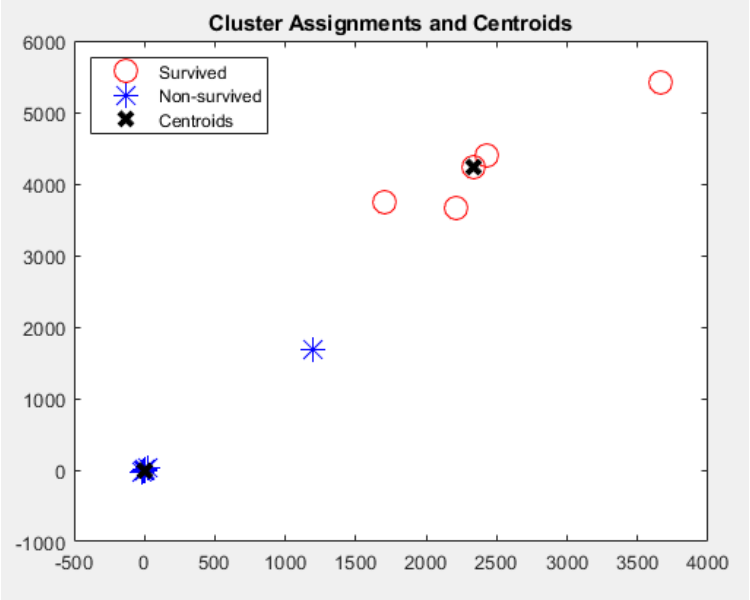

Figure 23: Clustering results of survived and non-survived patients

Table 4 summarized the clustering results of total population of 11 data points for both survived and non-serviced categories.

Table 4: summary of K-mean results

Total number of data points	11
True Negative (TN)	5
True Positive (TP)	3
False Positive (FP)	1
False Negative (FN)	2
Sensitivity=True Positive Rate= TP/(TP+FN)	60%
Accuracy= (TP+TN)/(TP+TN+FP+FN)	72%

To understand that whether F7 and F8 (significant channels from Entropy analysis) give us better clustering results relative to other channels or not, the same process applied for all available 16 channels.

The results were almost the same for all channels. It means we could not get any significant differences between channel 7 and 8 (Frontal channels) and other channels.

Note: Plots of the clustering results for all 16 channels are captured in Appendix I

8.6 More Analysis – Phase II

As a second level of processes, to increase the number of points of samples to cluster, every 15 minutes available data for each patients during hypothermia were extracted. Then a matrix was created that each rows represent every 15 minutes available data during hypothermia from all subjects. It means if we had 30 minutes of data for one survived patient, in that matrix we had two rows of 15 minutes for that patient. Then the SVD analysis applied on this matrix and data projection matrix on the 2 largest Eigen values were calculated. This way instead of 11 points on each figure, we had multiple data points from the same subject. Then all the data points were plotted. The data points from non-survived plotted with one color and from survived with another color. We Hypothesis that in the ideal scenario, the non-survived points should cluster together and the survived points should cluster together.

Here are summary of the analysis steps:

- re-sampled the data
- extracted all available 15 minutes of patients data during hypothermia

- generated a matrix with 37 rows (survived and un-survived samples), each rows contained 15 minutes of data
- applied the SVD analysis and plotted the projection matrix on the 2 largest Eigen values
- this matrix was created separately for each of 16 channels (16 plots)

This process were repeated for all 16 channels.

8.7 Results – Phase II

By increasing the number of data points from 11 to 37, there were no clear clustering for survived (red star *) and non-survived EEG samples (blue circles) in this set of analysis. Figure 24 and Figure 25 illustrate the clustering results for two channels of data.

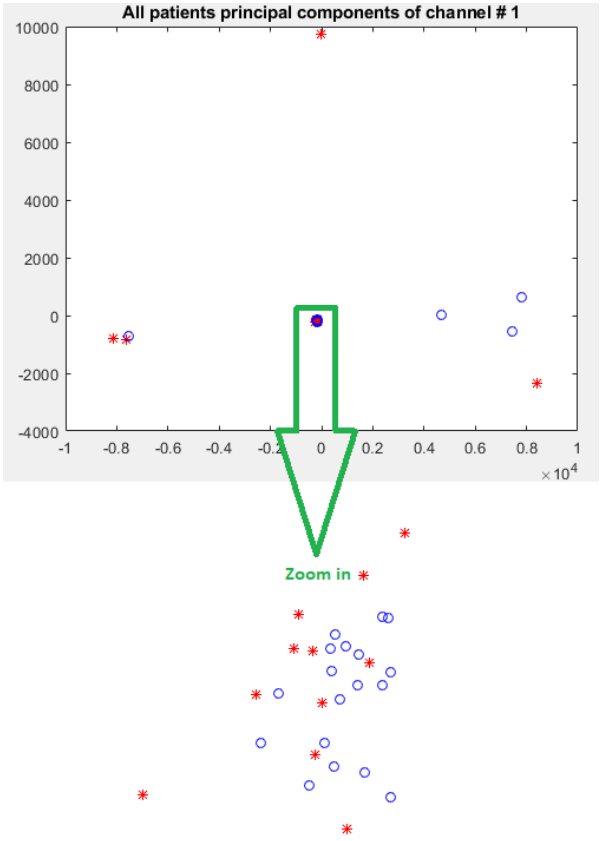

Figure 24: clustering result for channels 1 data points.

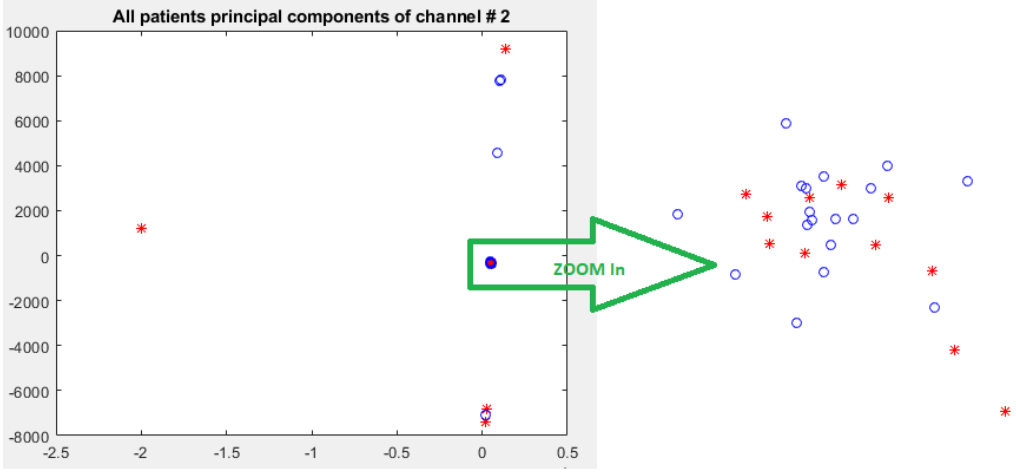

Figure 25: clustering result for channels 2 data points.

Note: Plots of the clustering results for all 16 channels are captured in Appendix II

8.8 Conclusion

The classic time dependent SVD analysis and K-mean clustering were not successful in categorizing data points from Survived and non-survived patients. This analysis confirms that Sub-band Wavelet Entropy (SWE) is a powerful method for EEG signals analysis during hypothermia. By using the SWE method, we were able to find the accurate frequency band of brain waves and the exact locations of the brain that have significant differences between survived and non-survived cardiac arrest patients.

APPENDIX I

Appendix I – Phase I plots

Plots of the clustering results of 11 data points for two Survived and non-survived categories for all available 16 EEG channels.

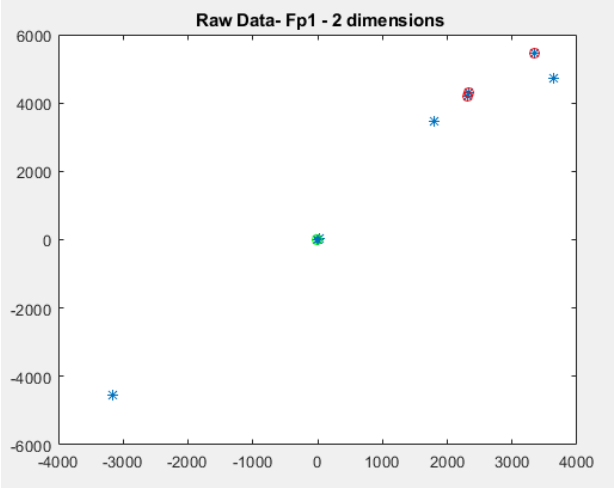

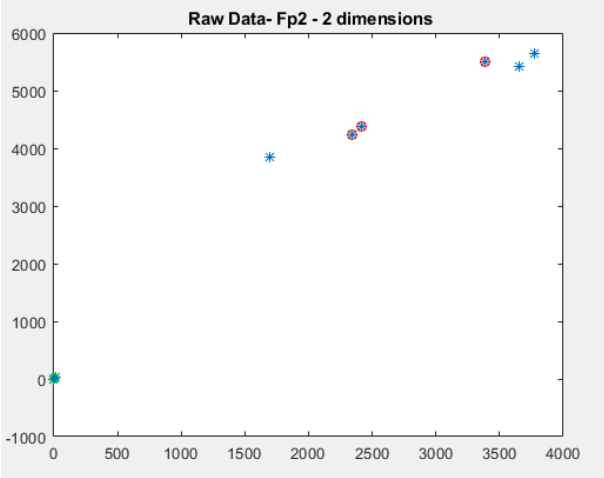

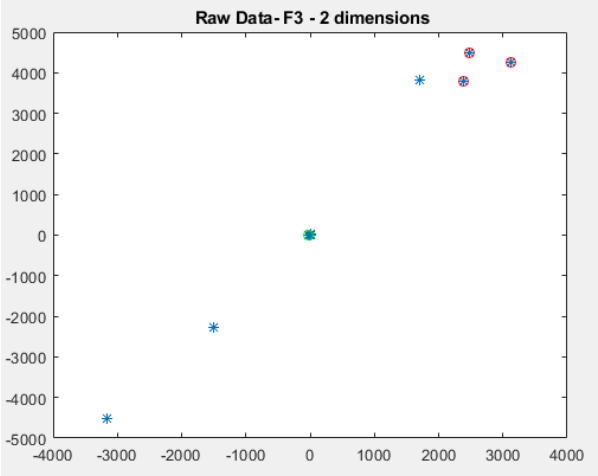

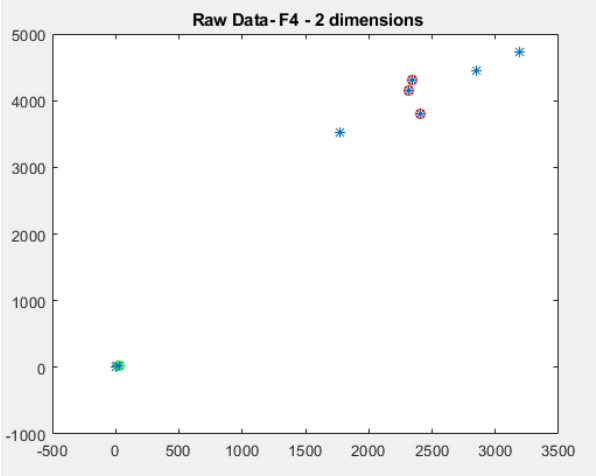

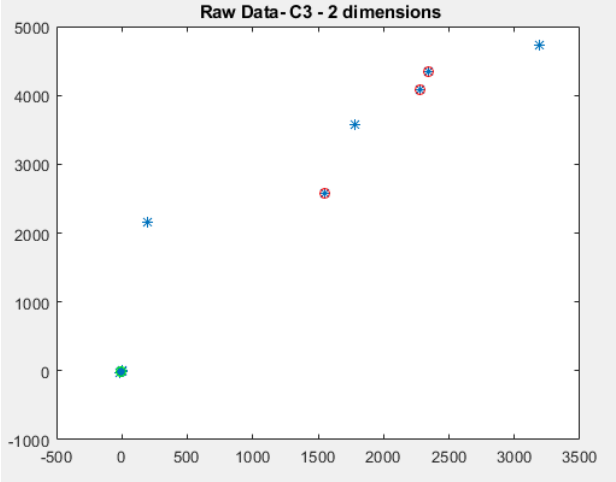
Raw Data- C3 - 2 dimensions
5000
4000
3000
2000
1000
0
-1000
-500
0
500
1000
1500
2000
2500
3000
3500

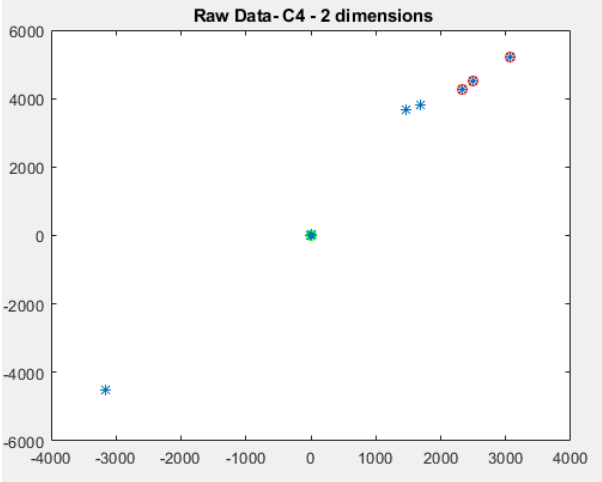
Raw Data- C4 - 2 dimensions
6000
4000
2000
0
-2000
-4000
-6000
-4000
-3000
-2000
-1000
0
1000
2000
3000
4000

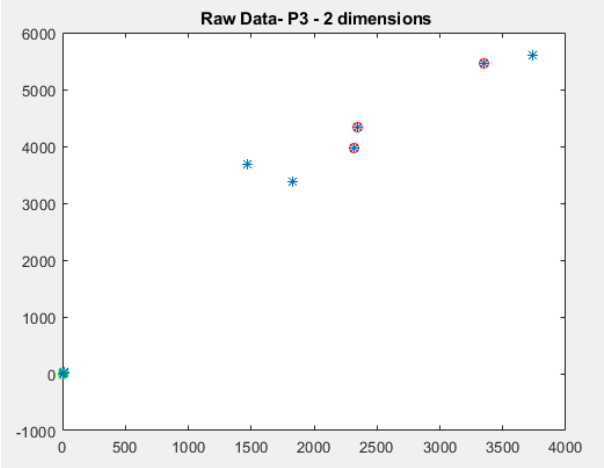
Raw Data- P3 - 2 dimensions
6000
5000
4000
3000
2000
1000
0
-1000
0
500
1000
1500
2000
2500
3000
3500
4000

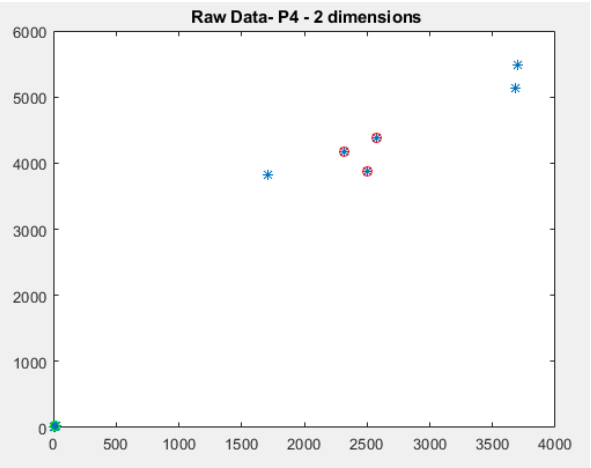
Raw Data- P4 - 2 dimensions
6000
5000
4000
3000
2000
1000
0
0
500
1000
1500
2000
2500
3000
3500
4000

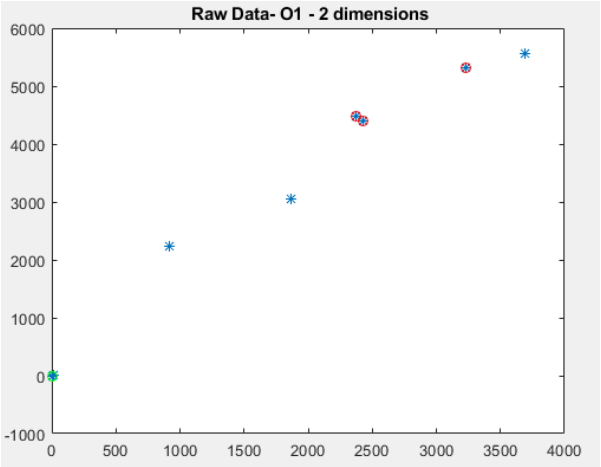
Raw Data- O1 - 2 dimensions
6000
5000
4000
3000
2000
1000
0
-1000
0
500
1000
1500
2000
2500
3000
3500
4000

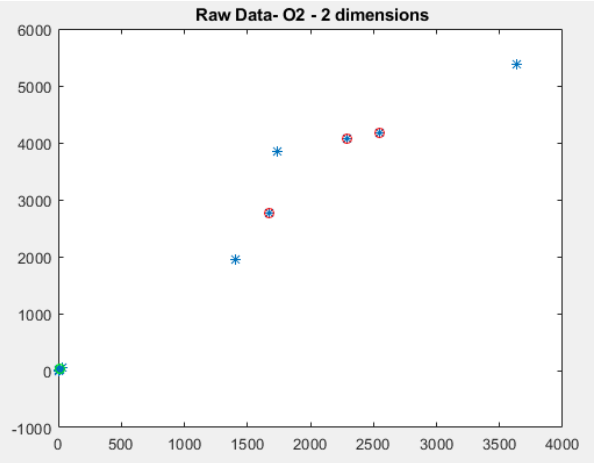
Raw Data- O2 - 2 dimensions
6000
5000
4000
3000
2000
1000
0
-1000
0
500
1000
1500
2000
2500
3000
3500
4000

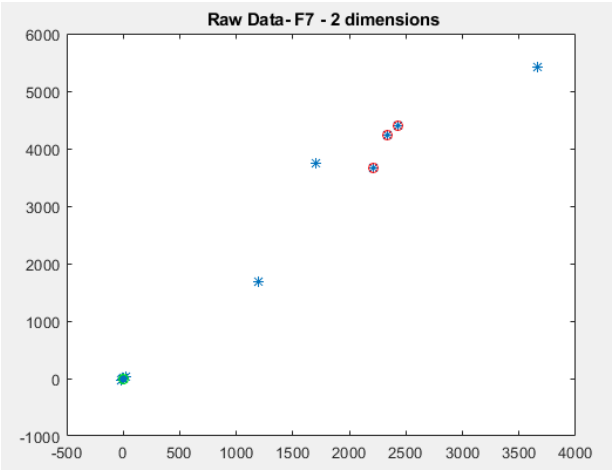
Raw Data- F7 - 2 dimensions
6000
5000
4000
3000
2000
1000
0
-1000
-500
0
500
1000
1500
2000
2500
3000
3500
4000

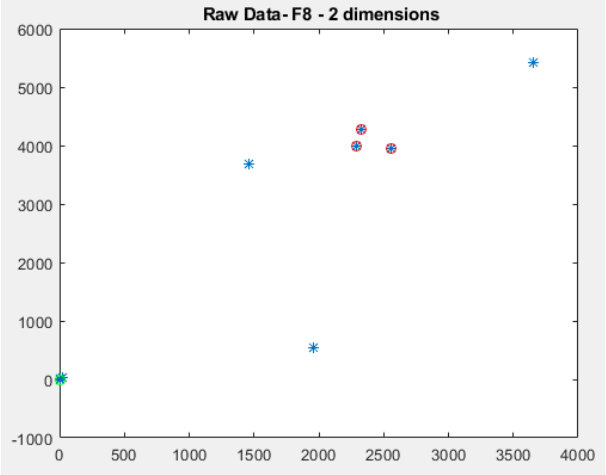
Raw Data- F8 - 2 dimensions
6000
5000
4000
3000
2000
1000
0
-1000
0
500
1000
1500
2000
2500
3000
3500
4000

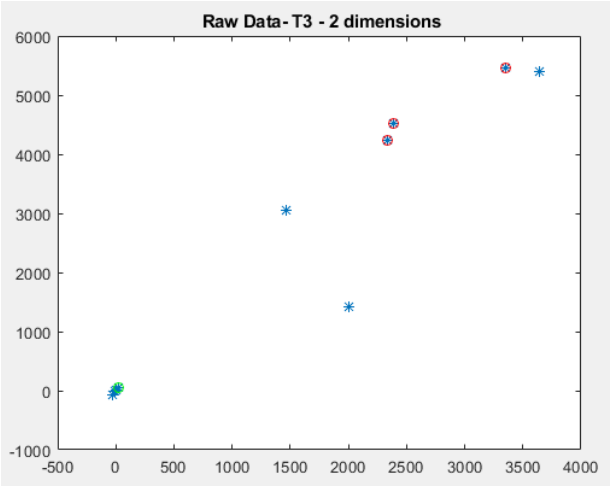
Raw Data- T3 - 2 dimensions
6000
5000
4000
3000
2000
1000
0
-1000
-500
0
500
1000
1500
2000
2500
3000
3500
4000

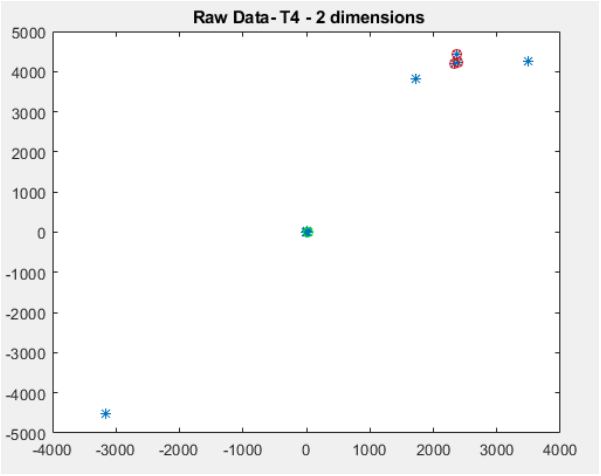
Raw Data- T4 - 2 dimensions
5000
4000
3000
2000
1000
0
-1000
-2000
-3000
-4000
-5000
-4000
-3000
-2000
-1000
0
1000
2000
3000
4000

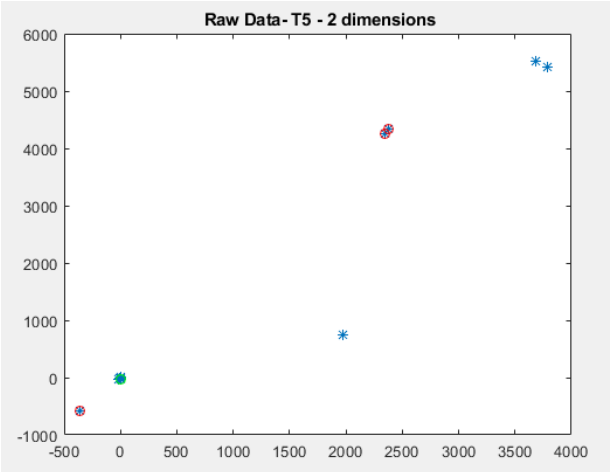
Raw Data- T5 - 2 dimensions
6000
5000
4000
3000
2000
1000
0
-1000
-500
0
500
1000
1500
2000
2500
3000
3500
4000

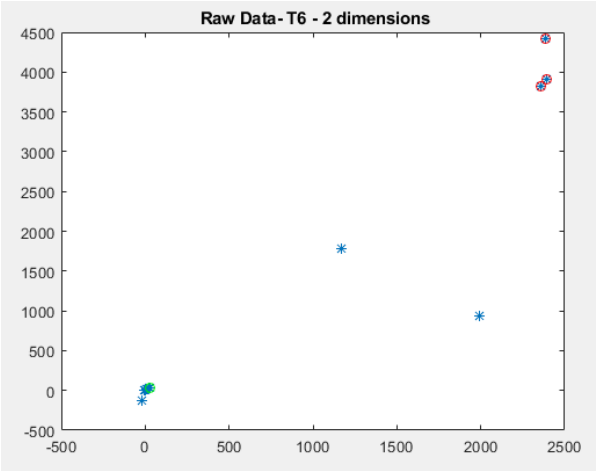
Raw Data- T6 - 2 dimensions
4500
4000
3500
3000
2500
2000
1500
1000
500
0
-500
-500
0
500
1000
1500
2000
2500

APPENDIX II

Appendix II – Phase II plots

Plots of the clustering results of 37 data points for two Survived and non-survived categories for all available 16 EEG channels.

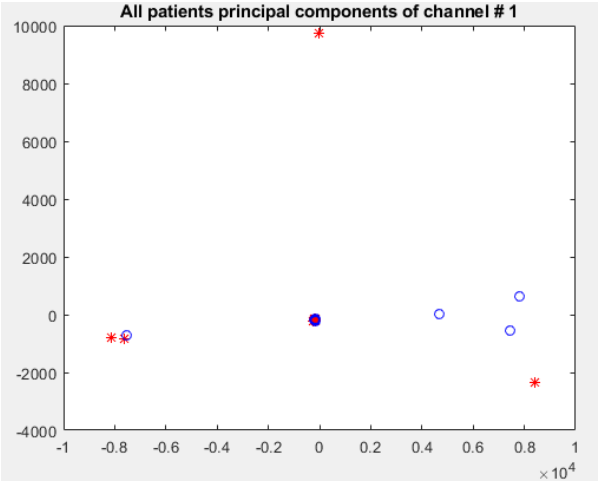

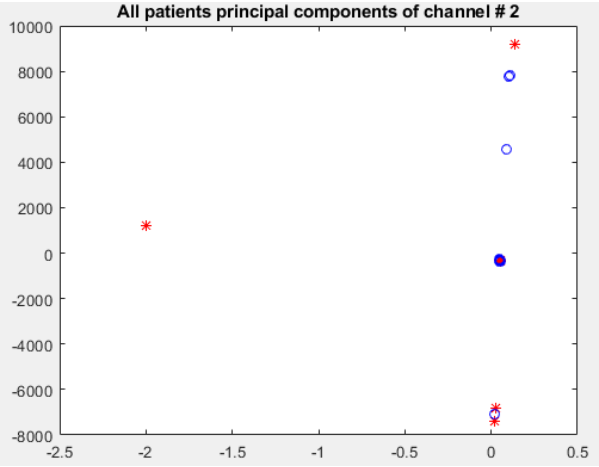

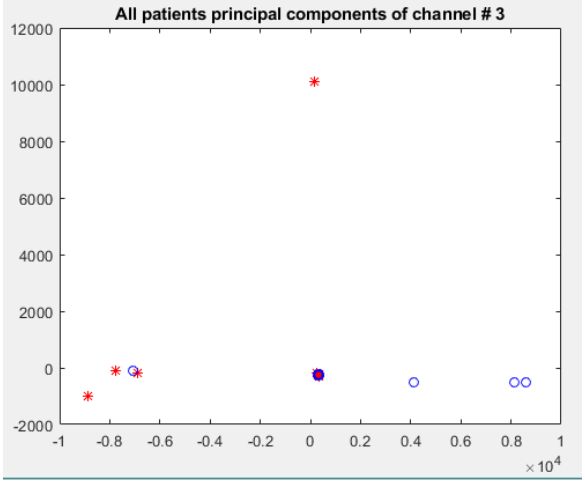

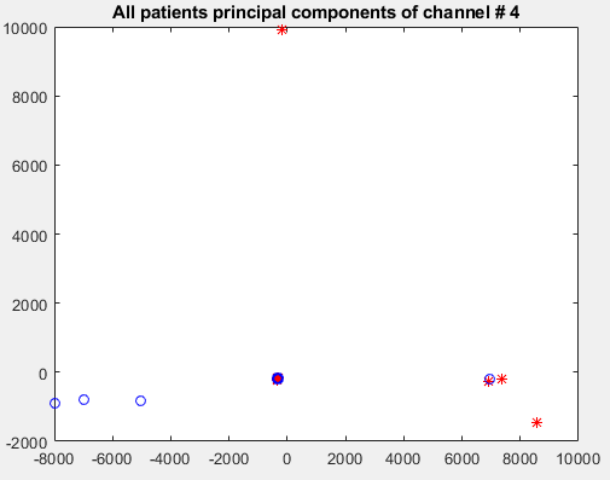

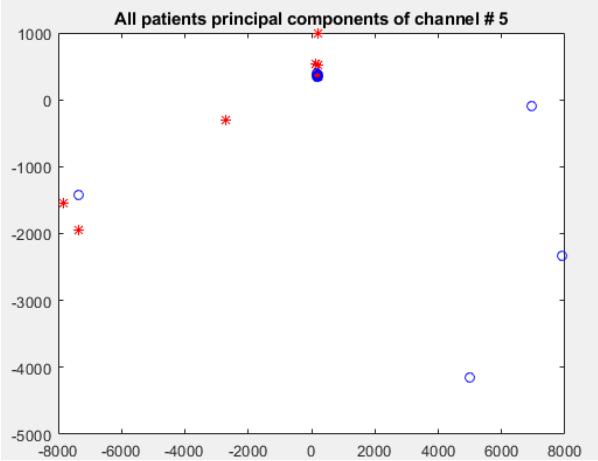
All patients principal components of channel # 5
1000
0
-1000
-2000
-3000
-4000
-5000
-8000
-6000
-4000
-2000
0
2000
4000
6000
8000

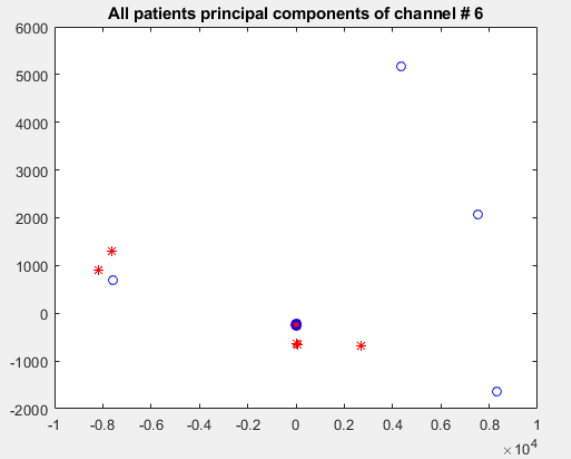
All patients principal components of channel # 6
6000
5000
4000
3000
2000
1000
0
-1000
-2000
-1
-0.8
-0.6
-0.4
-0.2
0
0.2
0.4
0.6
0.8
1
×10^4

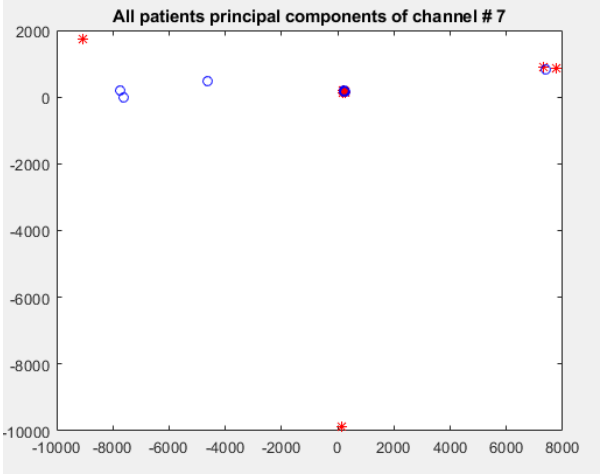
All patients principal components of channel # 7
2000
0
-2000
-4000
-6000
-8000
-10000
-10000
-8000
-6000
-4000
-2000
0
2000
4000
6000
8000

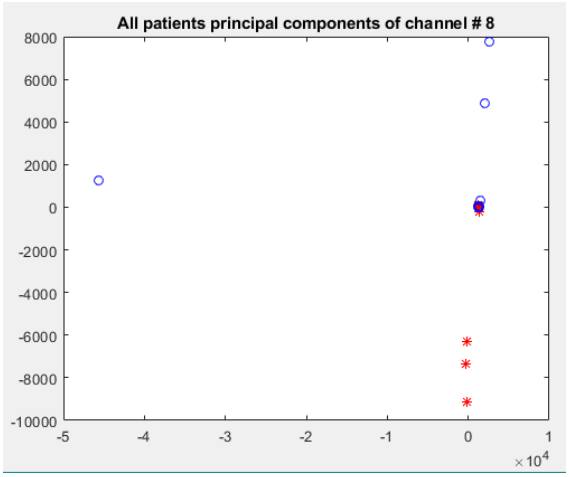
All patients principal components of channel # 8
8000
6000
4000
2000
0
-2000
-4000
-6000
-8000
-10000
-5
-4
-3
-2
-1
0
1
×10^4

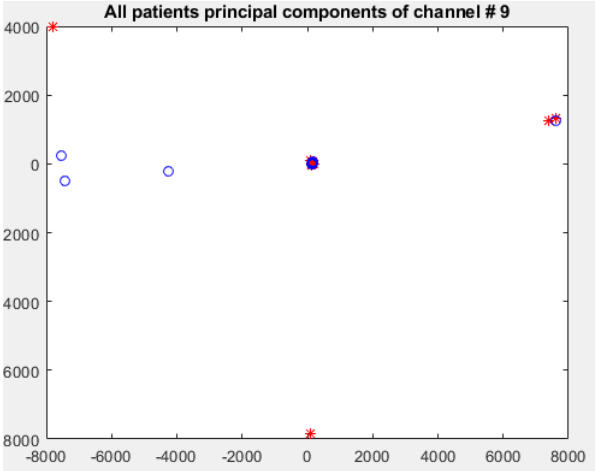
All patients principal components of channel # 9
4000
2000
0
2000
4000
6000
8000
-8000
-6000
-4000
-2000
0
2000
4000
6000
8000

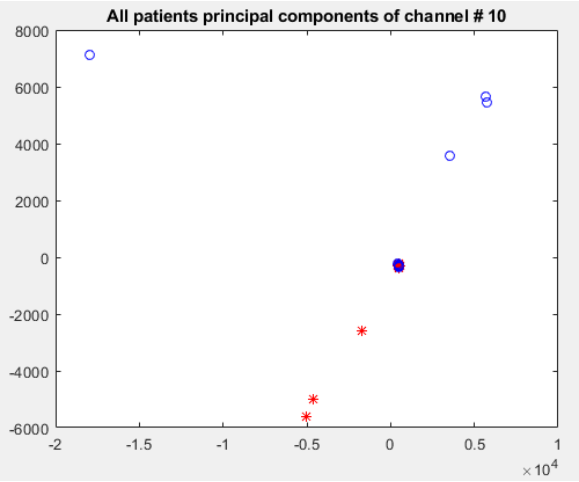
All patients principal components of channel # 10
8000
6000
4000
2000
0
-2000
-4000
-6000
-2
-1.5
-1
-0.5
0
0.5
1
×10^4

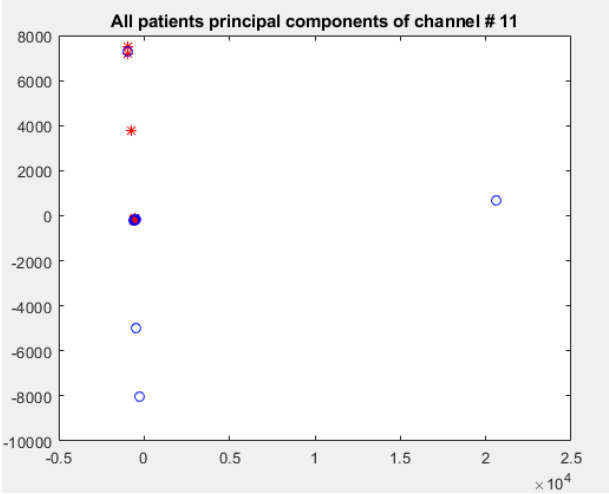
All patients principal components of channel # 11
8000
6000
4000
2000
0
-2000
-4000
-6000
-8000
-10000
-0.5
0
0.5
1
1.5
2
2.5
×10^4

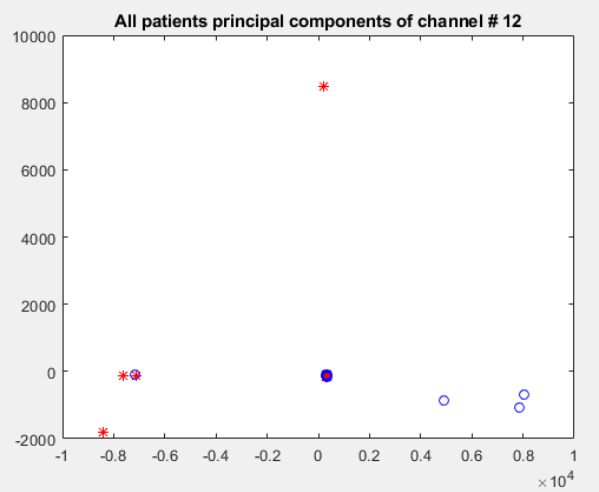
All patients principal components of channel # 12
10000
8000
6000
4000
2000
0
-2000
-1
-0.8
-0.6
-0.4
-0.2
0
0.2
0.4
0.6
0.8
1
×10^4

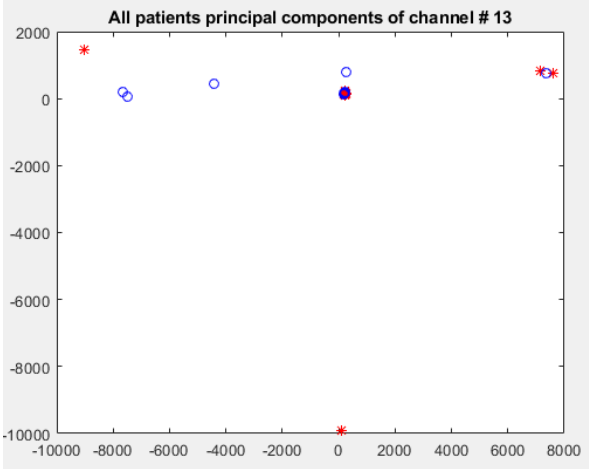
All patients principal components of channel # 13
2000
0
-2000
-4000
-6000
-8000
-10000
-10000
-8000
-6000
-4000
-2000
0
2000
4000
6000
8000

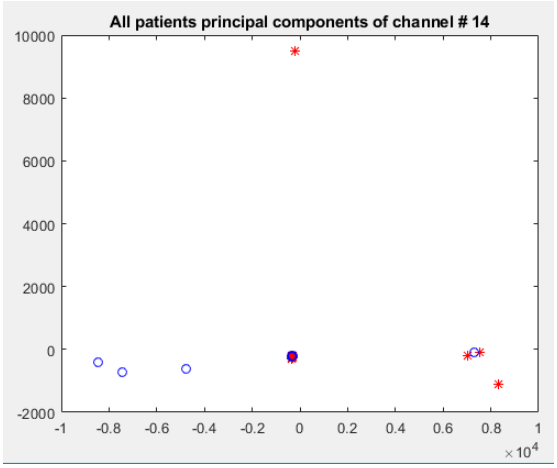
All patients principal components of channel # 14
10000
8000
6000
4000
2000
0
-2000
-1
-0.8
-0.6
-0.4
-0.2
0
0.2
0.4
0.6
0.8
1
×10^4

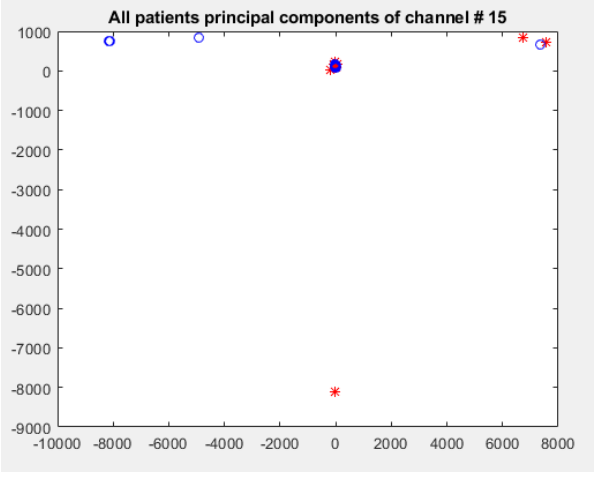
All patients principal components of channel # 15
1000
0
-1000
-2000
-3000
-4000
-5000
-6000
-7000
-8000
-9000
-10000
-8000
-6000
-4000
-2000
0
2000
4000
6000
8000

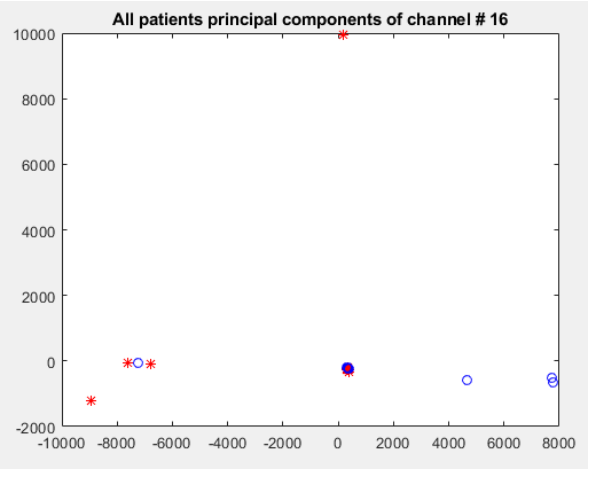
All patients principal components of channel # 16
10000
8000
6000
4000
2000
0
-2000
-10000
-8000
-6000
-4000
-2000
0
2000
4000
6000
8000

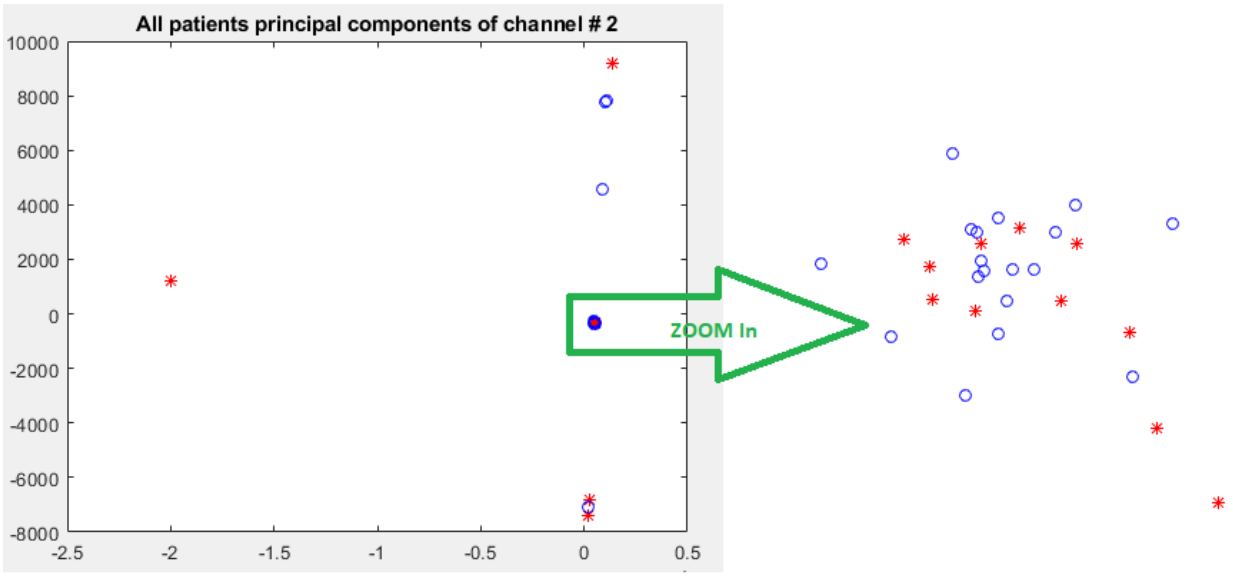
All patients principal components of channel # 2
10000
8000
6000
4000
2000
0
-2000
-4000
-6000
-8000
-2.5
-2
-1.5
-1
-0.5
0
0.5
ZOOM In

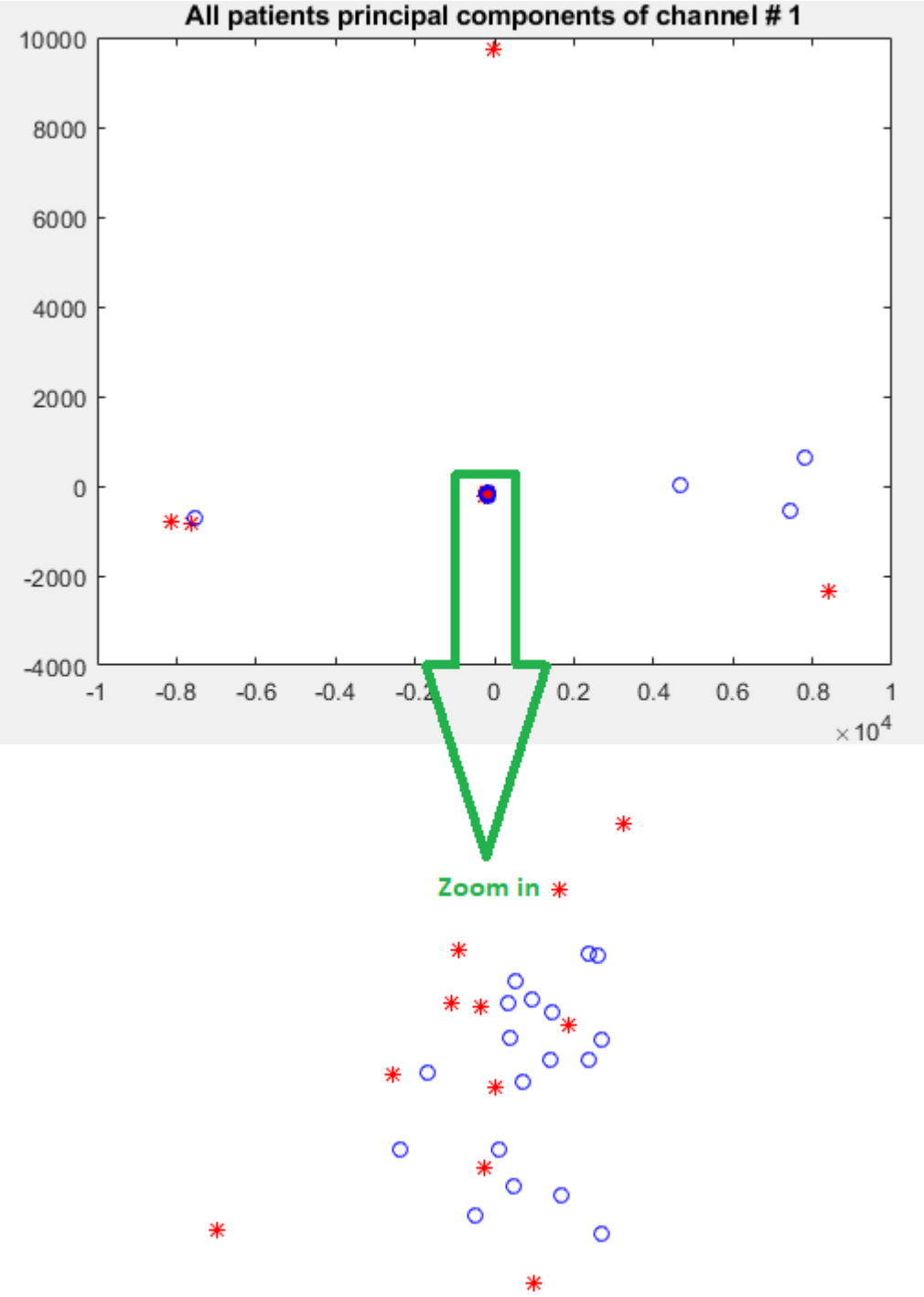
All patients principal components of channel # 1
10000
8000
6000
4000
2000
0
-2000
-4000
-1
-0.8
-0.6
-0.4
-0.2
0
0.2
0.4
0.6
0.8
1
×10^4
Zoom in

CHAPTER 9: REFERENCES

References

1. Nichol G, Thomas E, Callaway CW, Hedges J, Powell JL, Aufderheide TP, et al. Regional variation in out-of-hospital cardiac arrest incidence and outcome. JAMA. 2008;300:1423–31.

2. Stecker EC, Reinier K, Marijon E, Narayanan K, Teodorescu C, Uy-Evanado A, et al. Public health burden of sudden cardiac death in the United States. Circulation. 2014. https ://doi.org/10.1161/CIRCE P.113.00103 4

3. Loyd-Jones D, Adams RJ, Brown TM, Carnethon M, Dai S, De Simone G, et al. Executive summary: heart disease and stroke statistics—2010 update: a report from the American Heart Association. Circulation. 2010;121:948–54.

4. Mozaffarian D, Benjamin EJ, Go AS, Arnett DK, Blaha MJ, Cushman M, et al. Executive summary. Circulation. 2015;131:434–41.

5. Geocadin RG, Buitrago MM, Torbey MT, Chandra-Strobos N, Williams MA, Kaplan PW. Neurologic prognosis and withdrawal of life support after resuscitation from cardiac arrest. Neurology. 2006;67:105–8.

6. Lim C, Alexander MP, LaFleche G, Schnyer DM, Verfaellie M. The neurological and cognitive sequelae of cardiac arrest. Neurology. 2004;63:1774–8.

7. Samaniego EA, Persoon S, Wijman CA. Prognosis after cardiac arrest and hypothermia: a new paradigm. Curr Neurol Neurosci Rep. 2011;11:111–9.

8. Storm C, Steffen I, Schefold JC, Krueger A, Oppert M, Jörres A, et al. Mild therapeutic hypothermia shortens intensive care unit stay of survivors after out-of-hospital cardiac arrest compared to historical controls. Crit Care. 2008;12:R78.

9. Karapetkova M, Koenig MA, Jia X. Early prognostication markers in cardiac arrest patients treated with hypothermia. Euro J Neurol. 2015;23:476–88

10. Ghassemi MM, Amorim E, Pati SB, Mark RG, Brown EN, Purdon PL, et al. An enhanced cerebral recovery index for coma prognostication following cardiac arrest. In 2015 37th Annual International Conference of the IEEE Engineering in Medicine and Biology Society (EMBC), 2015, pp. 534–537.

11. Rossetti AO, Oddo M, Logroscino G, Kaplan PW. Prognostication after cardiac arrest and hypothermia: a prospective study. Ann Neurol. 2010;67:301–7.

12. Al Thenayan E, Savard M, Sharpe M, Norton L, Young B. Predictors of poor neurologic outcome after induced mild hypothermia following cardiac arrest. Neurology. 2008;71:1535–7.

13. Rundgren M, Westhall E, Cronberg T, Rosen I, Friberg H. Continuous amplitude-integrated electroencephalogram predicts outcome in hypothermia-treated cardiac arrest patients. Crit Care Med. 2010;38:1838–44.

14. Rittenberger JC, Popescu A, Brenner RP, Guyette FX, Callaway CW. Frequency and timing of nonconvulsive status epilepticus in comatose post-cardiac arrest subjects treated with hypothermia. Neurocrit Care. 2012;16:114–22.

15. Crepeau AZ, Rabinstein AA, Fugate JE, Mandrekar J, Wijdicks EF, White RD, et al. Continuous EEG in therapeutic hypothermia after cardiac arrest Prognostic and clinical value. Neurology.2013;80:339–44.

16. Snyder BD, Hauser WA, Loewenson RB, Leppik IE, Ramirez- Lassepas M, Gumnit RJ. Neurologic prognosis after cardiopulmonary arrest: III. Seizure activity. Neurology. 1980;30:1292–7.

17. Wijdicks EF, Hijdra A, Young GB, Bassetti CL, Wiebe S. Practice parameter: prediction of outcome in comatose survivors after cardiopulmonary resuscitation (an evidence-based review): report of the Quality Standards Subcommittee of the American Academy of Neurology. Neurology. 2006;67:203–10.

18. Moshirvaziri H, Ramezan-Arab N, Asgari S Prediction of the outcome in cardiac arrest patients undergoing hypothermia using EEG wavelet entropy. In 2016 38th Annual International Conference of the IEEE Engineering in Medicine and Biology Society (EMBC), 2016, pp. 3777–80.

19. Jia X, Koenig MA, Nickl R, Zhen G, Thakor NV, Geocadin RG. Early electrophysiologic markers predict functional outcome associated with temperature manipulation after cardiac arrest in rats. Crit Care Med. 2008;36:1909–16.

20. Koenig MA, Kaplan PW, Thakor NV. Clinical neurophysiologic monitoring and brain injury from cardiac arrest. Neurol Clin. 2006;24:89–106.

21. Wennervirta JE, Ermes MJ, Tiainen SM, Salmi TK, Hynninen MS, Sarkela MO, et al. Hypothermia-treated cardiac arrest patients with good neurological outcome differ early in quantitative variables of EEG suppression and epileptiform activity". Crit Care Med. 2009;37:2427–35.

22. Viertio-Oja H, Maja V, Sarkela M, Talja P, Tenkanen N, Tolvanen- Laakso H, et al., Description of the entropy algorithm as applied in the Datex-Ohmeda S/5 entropy module. Acta Anaesthesiol

Scand. 2004;48:154–61.

23. Yang Q, Su Y, Hussain M, Chen W, Ye H, Gao D, et al. Poor outcome prediction by burst suppression ratio in adults with postanoxic coma without hypothermia. Neurol Res. 2014. https ://doi. org/10.1179/17431 32814 Y.00000 00346 .

24. Levy WJ, Pantin E, Mehta S, McGarvey M. Hypothermia the approximate entropy of the electroencephalogram. Anesthesiology. 2003;98:53–7.

25. Jia X, Koenig MA, Shin HC, Zhen G, Yamashita S, Thakor NV, et al., Quantitative EEG and neurological recovery with therapeutic hypothermia after asphyxial cardiac arrest in rats. Brain Res. 2006;1111:166–75.

26. Kang X, Jia X, Geocadin RG, Thakor NV, Maybhate A. Multiscale entropy analysis of EEG for assessment of post-cardiac arrest neurological recovery under hypothermia in rats. IEEE Trans Biomed Eng. 2009;56:1023–31.

27. Dandan Z, Jia X, Ding H, Ye D, Thakor NV. Application of Tsallis entropy to EEG: quantifying the presence of burst suppression after asphyxial cardiac arrest in rats. IEEE Trans Biomed Eng. 2010;57:867–74.

28. Noirhomme Q, Lehembre R, Lugo Zdel R, Lesenfants D, Luxen A, Laureys S, et al. Automated analysis of background EEG and reactivity during therapeutic hypothermia in comatose patients after cardiac arrest. Clin EEG Neurosci. 2014;45:6–13.

29. Deboer T. Brain temperature dependent changes in the electroencephalogram power spectrum of humans and animals. J Sleep Res. 1998;7:254–62.

30. Borda M. Fundamentals in information theory and coding. Berlin: Springer; 2011.

31. Seely AJ, Macklem PT. Complex systems and the technology of variability analysis. Crit Care. 2004;8:R367.

32. Tong S, Bezerianos A, Paul J, Zhu Y, Thakor N. Nonextensive entropy measure of EEG following brain injury from cardiac arrest". Phys A. 2002;305:619–28.

33. Chen B, Song FQ, Sun LL, Lei LY, Gan WN, Chen MH, et al., Improved early postresuscitation EEG activity for animals treated with hypothermia predicted 96 hr neurological outcome and survival in a rat model of cardiac arrest. Biomed Res Int. 2013. https ://doi.org/10.1155/2013/31213 7

34. Ajam K, Gold LS, Beck SS, Damon S, Phelps R, Rea TD. Reliability of the Cerebral Performance Category to classify neurological status among survivors of ventricular fibrillation arrest: a cohort study. Scand J Trauma Resusc Emerg Med. 2011;19:38.

35. Ho KK, Moody GB, Peng CK, Mietus JE, Larson MG, Levy D, et al. Predicting survival in heart failure case and control subjects by use of fully automated methods for deriving nonlinear and conventional indices of heart rate dynamics. Circulation. 1997;96:842–8.

36. Pincus SM Approximate entropy as a measure of system complexity. Proc Natl Acad Sci. 1991;88:2297–2301.

37. Grassberger P. Information and complexity measures in dynamical systems in Information dynamics. New York: Springer; 1991, pp. 15–33.

38. Costa M, Goldberger AL, Peng C-K. Multiscale entropy analysis of complex physiologic time series. Phys Rev Lett. 2002;89:068102.

39. Richman JS, Moorman JR. Physiological time-series analysis using approximate entropy and sample entropy. Am J Physiol Heart Circ Physiol. 2000;278:H2039–49.

40. Steriade M, Llinás RR. The functional states of the thalamus and the associated neuronal interplay. Physiol Rev. 1988;68:649–742.

41. Katz L, Ebmeyer U, Safar P, Radovsky A, Neumar R. Outcome model of asphyxial cardiac arrest in rats. J Cereb Blood Flow Metab. 1995;15:1032–9.

42. Geocadin R, Ghodadra R, Kimura T, Lei H, Sherman D, Hanley D, et al. A novel quantitative EEG injury measure of global cerebral ischemia. Clin Neurophysiol. 2000;111:1779–87.

43. Shen EH, Cai ZJ, Gu FJ. Mathematical foundation of a new complexity measure. Appl Math Mech. 2005;26:1188–96.

44. Lu Y, Jiang D, Jia X, Qiu Y, Zhu Y, Thakor N, et al. Predict the neurological recovery under hypothermia after cardiac arrest using C0 complexity measure of EEG signals. In Engineering in Medicine and Biology Society, 2008. EMBS 2008. 30th Annual International Conference of the IEEE, 2008, pp. 2133–6.

45. Sarkela MO, Ermes MJ, van Gils MJ, Yli-Hankala AM, Jantti VH, Vakkuri AP. Quantification of epileptiform electroencephalographic activity during sevoflurane mask induction. Anesthesiology. 2007;107:928–38.

46. Bhattacharyya S, Biswas A, Mukherjee J, Majumdar AK, Majumdar B, Mukherjee S, et al. Detection of artifacts from high energy bursts in neonatal EEG. Comput Biol Med. 2013;43:1804–14.

47. Sarkela M, Mustola S, Seppanen T, Koskinen M, Lepola P, Suominen K, et al. Automatic analysis and monitoring of burst suppression in anesthesia. J Clin Monit Comput. 2002;17:125–34.

48. Seder DB, Dziodzio J, Smith KA, Hickey P, Bolduc B, Stone P, et al. Feasibility of bispectral index monitoring to guide early postresuscitation cardiac arrest triage. Resuscitation. 2014;85:1030–6.

49. Shin H-C, Tong S, Yamashita S, Jia X, Geocadin G, Thakor V. Quantitative EEG and effect of hypothermia on brain recovery after cardiac arrest. IEEE Trans Biomed Eng. 2006;53:1016–23.

50. Shin H-C, Jia X, Nickl R, Geocadin RG, Thakor NV. A subband- based information measure of EEG during brain injury and recovery after cardiac arrest. IEEE Trans Biomed Eng. 2008;55:1985–90.

51. Jia X, Koenig MA, Shin H-C, Zhen G, Pardo CA, Hanley DF, et al. Improving neurological outcomes post-cardiac arrest in a rat model: immediate hypothermia and quantitative EEG monitoring. Resuscitation. 2008;76:431–42.

52. Deng R, Young LM, Jia X. Quantitative EEG markers in severe post-resuscitation brain injury with therapeutic hypothermia. In Engineering in Medicine and Biology Society (EMBC), 2015 37th Annual International Conference of the IEEE, 2015, pp. 6598–601.

53. Deng R, Koenig MA, Young LM, Jia X. Early quantitative gamma-band EEG marker is associated with outcomes after cardiac arrest and targeted temperature management. Neurocrit. Care. 2015;23:262–73.

54. Tjepkema-Cloostermans MC, van Meulen FB, Meinsma G, van Putten MJ. A Cerebral Recovery Index (CRI) for early prognosis in patients after cardiac arrest. Crit Care. 2013;17:1.

55. Tsallis C. Possible generalization of Boltzmann-Gibbs statistics. J Stat Phys. 1988;52:479–87.

56. Contreras D, Destexhe A, Sejnowski TJ, Steriade M. Spatiotemporal patterns of spindle oscillations in cortex and thalamus. J Neurosci. 1997;17:1179–96.

57. Zhang D, Jia X, Ding H, Ye D, Thakor NV. Application of Tsallis entropy to EEG: quantifying the presence of burst suppression after asphyxial cardiac arrest in rats. IEEE Trans Biomed Eng. 2010;57:867–74.

58. Proakis JG, Manolakis DG. Digital signal processing (4th ed.). Upper Saddle River, N.J.: Pearson Prentice Hall; 2007. 59. Stam CJ, Nolte G, Daffertshofer A. Phase lag index: assessment of functional connectivity from multi channel EEG and MEG with diminished bias from common sources. Human Brain Mapp. 2007;28:1178–93.

60. Seder DB, Fraser GL, Robbins T, Libby L, Riker RR. The bispectral index and suppression ratio are very early predictors of neurological outcome during therapeutic hypothermia after cardiac arrest. Intensive Care Med. 2010;36:281–8.

61. Leary M, Fried DA, Gaieski DF, Merchant RM, Fuchs BD, Kolansky DM, et al. Neurologic prognostication and bispectral index monitoring after resuscitation from cardiac arrest. Resuscitation. 2010;81:1133–7, .

62. Riker RR, Stone PC Jr, May T, McCrum B, Fraser GL, Seder D. Initial bispectral index may identify patients who will awaken during therapeutic hypothermia after cardiac arrest: a retrospective pilot study. Resuscitation. 2013;84:794–7.

63. Selig C, Riegger C, Dirks B, Pawlik M, Seyfried T, Klingler W. Bispectral index (BIS) and suppression ratio (SR) as an early predictor of unfavourable neurological outcome after cardiac arrest. Resuscitation. 2014;85:221–6.

64. Stammet P, Wagner DR, Gilson G, Devaux Y. Modeling serum level of s100beta and bispectral index to predict outcome after cardiac arrest. J Am Coll Cardiol. 2013;62:851–8.

65. Stammet P, Collignon O, Werer C, Sertznig C, Devaux Y. Bispectral index to predict neurological outcome early after cardiac arrest. Resuscitation. 2014;85:1674–80.

66. Jouffroy R, Lamhaut L, Guyard A, Philippe P, An K, Spaulding C, et al. Early detection of brain death using the Bispectral Index (BIS) in patients treated by extracorporeal cardiopulmonary resuscitation (E-CPR) for refractory cardiac arrest. Resuscitation. 2017;120:8–13.

67. Ochiai K, Shiraishi A, Otomo Y, Koido Y, Kanemura T, Honma M. Increasing or fluctuating bispectral index values during postresuscitation targeted temperature management can predict clinical seizures after rewarming. Resuscitation. 2017;114:106–12.

68. Levy DE, Caronna JJ, Singer BH, Lapinski RH, Frydman H, Plum F. Predicting outcome from hypoxic-lschemic coma. JAMA. 1985;253:1420–6.

69. Zandbergen E, Hijdra A, Koelman J, Hart A, Vos P, Verbeek M, et al. Prediction of poor outcome within the first 3 days of postanoxic coma. Neurology. 2006;66:62–8.

70. Anand N, Stead LG. Neuron-specific enolase as a marker for acute ischemic stroke: a systematic review. Cerebrovasc Dis. 2005;20:213–9.

71. Scheel M, Storm C, Gentsch A, Nee J, Luckenbach F, Ploner CJ, et al. The prognostic value of gray-white-matter ratio in cardiac arrest patients treated with hypothermia. Scand J Trauma, Resusc Emerg Med. 2013;21:23.

72. Rudolf J, Ghaemi M, Ghaemi M, Haupt WF, Szelies B, Heiss W-D. Cerebral glucose metabolism in acute and persistent vegetative state. J Neurosurg Anesthesiol. 1999;11:17–24.

73. Welsh FA, Sims RE, Harris VA. Mild hypothermia prevents ischemic injury in gerbil hippocampus. J Cereb Blood Flow Metab. 1990;10:557–63.

74. Minamisawa H, Smith ML, Siesjo BK. The effect of mild hyperthermia and hypothermia on brain damage following 5, 10, and 15 minutes of forebrain ischemia. Ann Neurol. 1990;28:26–33.

75. Bernard SA, Gray TW, Buist MD, Jones BM, Silvester W, Gutteridge G, et al. Treatment of comatose survivors of out-of-hospital cardiac arrest with induced hypothermia. N Engl J Med. 2002;346:557–63.

76. Fugate JE, Wijdicks EF, Mandrekar J, Claassen DO, Manno EM, White RD, et al. Predictors of neurologic outcome in hypothermia after cardiac arrest. Ann Neurol. 2010;68:907–14. 77. Deakin CD, Nolan JP, Soar J, Sunde K, Koster RW, Smith GB, et al. European resuscitation council guidelines for resuscitation 2010 Sect. 4. Adult advanced life support. Resuscitation. 2010;81:1305–52.

78. Cloostermans MC, van Meulen FB, Eertman CJ, Hom HW, van Putten MJ. Continuous electroencephalography monitoring for early prediction of neurological outcome in postanoxic patients after cardiac arrest: a prospective cohort study. Crit Care Med. 2012;40:2867–75.

79. D. Ruoxian, L. M. Young, and J. Xiaofeng, "Quantitative EEG markers in severe post-resuscitation brain injury with therapeutic hypothermia," in Engineering in Medicine and Biology Society (EMBC), 2015 37th Annual International Conference of the IEEE, 2015, pp. 6598-6601.

80. X. Jia, M. A. Koenig, R. Nickl, G. Zhen, N. V. Thakor, and R. G. Geocadin, "Early electrophysiologic markers predict functional outcome associated with temperature manipulation after cardiac arrest in rats," Crit Care Med, vol. 36, pp. 1909- 16, Jun 2008.

81. X. Jia, M. A. Koenig, H. C. Shin, G. Zhen, S. Yamashita, N. V. Thakor, et al., "Quantitative EEG and neurological recovery with therapeutic hypothermia after asphyxial cardiac arrest in rats," Brain Res, vol. 1111, pp. 166-75, Sep 21 2006.

82. Z. Dandan, X. Jia, H. Ding, D. Ye, and N. V. Thakor, "Application of Tsallis entropy to EEG: quantifying the presence of burst suppression after asphyxial cardiac arrest in rats," IEEE Trans Biomed Eng, vol. 57, pp. 867-74, Apr 2010.

83. M. O. Sarkela, M. J. Ermes, M. J. van Gils, A. M. Yli- Hankala, V. H. Jantti, and A. P. Vakkuri, "Quantification of epileptiform electroencephalographic activity during sevoflurane mask induction," Anesthesiology, vol. 107, pp.

928-38, Dec 2007.

84. F. Darvas, R. Scherer, J. G. Ojemann, R. P. Rao, K. J. Miller, and L. B. Sorensen, "High gamma mapping using EEG," Neuroimage, vol. 49, pp. 930-8, Jan 1 2010.

85. Q. Noirhomme, R. Lehembre, R. Lugo Zdel, D. Lesenfants, A. Luxen, S. Laureys, et al., "Automated analysis of background EEG and reactivity during therapeutic hypothermia in comatose patients after cardiac arrest," Clin EEG Neurosci, vol. 45, pp. 6-13, Jan 2014.

86. J. E. Wennervirta, M. J. Ermes, S. M. Tiainen, T. K. Salmi, M. S. Hynninen, M. O. Sarkela, et al., "Hypothermia-treated cardiac arrest patients with good neurological outcome differ early in quantitative variables of EEG suppression and epileptiform activity," Crit Care Med, vol. 37, pp. 2427-35, Aug 2009.

87. D. Wu, A. Bezerianos, H. Zhang, X. Jia, and N. V. Thakor, "Exploring high-frequency oscillation as a marker of brain ischemia using S-transform," Conf Proc IEEE Eng Med Biol Soc, vol. 2010, pp. 6099-102, 2010.

88. C. Endisch, C. Storm, C. J. Ploner, and C. Leithner, "Somatosensory evoked high-frequency oscillations and prognostication after cardiac arrest," Critical Care, vol. 19, pp. P431-P431, 03/16 2015.

89. A. Mirzaei, A. Ayatollahi, H, "Statistical analysis of epileptic activities based on histogram and wavelet-spectral entropy," Journal of Biomedical Science and Engineering. 2011 Mar 8;4(03):207.

90. EEG: Origin and Measurement; F. Lopes da Silva: Centre of Neurosciences, Swammerdam Institute for Life Sciences, University of Amsterdam , Kruislaan 320 , 1098 , SM Amsterdam , The Netherlands e-mail: silva@science.uva.nl [Mulert, C., & Lemieux, L. (Eds.). (2009). EEG-fMRI: physiological basis, technique, and applications. Springer Science & Business Media.]

91. Bronzino, Joseph D. Biomedical engineering handbook. Vol. 2. CRC press, 1999.

92. Teplan, M. (2002). Fundamentals of EEG measurement. Measurement science review, 2(2), 1-11.

93. Survey on EEG Signal Processing Methods; M. Rajya Lakshmi, Dr. T. V. Prasad, Dr. V. Chandra Prakash; International Journal of Advanced Research in Computer Science and Software Engineering; Volume 4, Issue 1, January 2014

94. Klimesch, W. (1999). EEG alpha and theta oscillations reflect cognitive and memory performance: a review and analysis. Brain research reviews, 29(2), 169-195.

95. Subha, D. P., Joseph, P. K., Acharya, R., & Lim, C. M. (2010). EEG signal analysis: a survey. Journal of medical systems, 34(2), 195-212.

96. Sanei, S., & Chambers, J. A. (2013). EEG signal processing. John Wiley & Sons.

97. Tjepkema-Cloostermans, M. C., van Meulen, F. B., Meinsma, G., & van Putten, M. J. (2013). A Cerebral Recovery Index (CRI) for early prognosis in patients after cardiac arrest. Crit Care, 17, R252.

98. Chhaganlal, K., 2014. Diagnosis and differential diagnosis of meningitis at patient's bed side using urine reagent strip to evaluate cerebro spinal fluid (Doctoral dissertation, lmu).

99. American Heart Association: Heart Attack or Sudden Cardiac Arrest: How Are They Different? (July 31, 2015) Retrieved from: https://www.heart.org/en/health-topics/heart-attack/about-heart-attacks/heart-attack-or-sudden-cardiac-arrest-how-are-they-different

100. Sanders, A. B. (2006). Therapeutic hypothermia after cardiac arrest. Current opinion in critical care, 12(3), 213-217.

101. Ermes, M., Sarkela, M., van Gils, M., Wennervirta, J., Vakkuri, A., & Salmi, T. (2007, August). Prediction of poor outcome using detector of epileptiform EEG in ICU patients resuscitated after cardiac

arrest. In Engineering in Medicine and Biology Society, 2007. EMBS 2007. 29th Annual International Conference of the IEEE (pp. 3056-3059). IEEE

102. Jia, Xiaoxuan, and Adam Kohn. "Gamma rhythms in the brain." PLoS biology 9, no. 4 (2011): e1001045.

103. Soleimanpour, H., Rahmani, F., Safari, S., & Golzari, S.E. (2014). Hypothermia After Cardiac Arrest as a Novel Approach to Increase Survival in Cardiopulmonary Cerebral Resuscitation: A Review. Iranian Red Crescent medical journal.

104. Georgieva, Petia, Filipe Silva, Mariofanna Milanova, and Nikola Kasabov. "EEG Signal Processing for Brain–Computer Interfaces." In Springer Handbook of Bio-/Neuroinformatics, pp. 797-812. Springer, Berlin, Heidelberg, 2014.

105. Ghiyamat, A., Shafri, H.Z.M., Mahdiraji, G.A., Ashurov, R., Shariff, A.R.M. and Mansor, S., 2014. Impact of discrete wavelet transform on discriminating airborne hyperspectral tropical rainforest tree species. Journal of Applied Remote Sensing, 8(1), p.083556.

106. MathWorks Statistics Toolbox: User's Guide (R2018b)

107. Glass, G.V., P.D. Peckham, and J.R. Sanders. 1972. Consequences of failure to meet assumptions underlying fixed effects analyses of variance and covariance. Rev. Educ. Res. 42: 237-288.

108. Harwell, M.R., E.N. Rubinstein, W.S. Hayes, and C.C. Olds. 1992. Summarizing Monte Carlo results in methodological research: the one- and two-factor fixed effects ANOVA cases. J. Educ. Stat. 17: 315-339.

109. Lix, L.M., J.C. Keselman, and H.J. Keselman. 1996. Consequences of assumption violations revisited: A quantitative review of alternatives to the one-way analysis of variance F test. Rev. Educ. Res. 66: 579-619.

110. Kumar, S. Pravin, N. Sriraam, and P. G. Benakop. "Automated detection of epileptic seizures using wavelet entropy feature with recurrent neural network classifier." In TENCON 2008-2008 IEEE Region 10 Conference, pp. 1-5. IEEE, 2008.

111. Liu, Boqiang, Junbo Gao, Zhongguo Liu, Zhenwang Zhang, Cong Yin, Cuiping Peng, and Jason Gu. "Brainwave classification based on wavelet entropy and event-related desynchronization." In 2007 Canadian Conference on Electrical and Computer Engineering, pp. 1018-1021. IEEE, 2007.

112. Mark S.Scher , Pediatric Neurophysiologic Evaluation (Chapter 13), Swaiman's Pediatric Neurology (Sixth Edition) 2017, Pages 87-96

113. Juri D.Kropotov , Frontal Midline Theta Rhythm (Chapter 2.4) , Functional Neuromarkers for Psychiatry, Applications for Diagnosis and Treatment, 2016, Pages 121-133

114. Grunwald, M., Weiss, T., Krause, W., Beyer, L., Rost, R., Gutberlet, I. and Gertz, H.J., 1999. Power of theta waves in the EEG of human subjects increases during recall of haptic information. Neuroscience Letters, 260(3), pp.189-192.

115. Hedna, V.S., Bodhit, A.N., Ansari, S., Falchook, A.D., Stead, L., Heilman, K.M. and Waters, M.F., 2013. Hemispheric differences in ischemic stroke: is left-hemisphere stroke more common?. Journal of Clinical Neurology, 9(2), pp.97-102.

116. Jason Brownlee, PhD. Machine learning mastery, LLinear Algebra, Introduction to Singular-Value Decomposition for Machine Learning (February 26, 2018. (Retrieved from: https://machinelearningmastery.com/singular-value-decomposition-for-machine-learning/)

117. MathWorks Statistics and Machine Learning Toolbox: User's Guide (R2018b)

118. Asgari, S., Moshirvaziri, H., Scalzo, F. and Ramezan-Arab, N., 2018. Quantitative measures of EEG for prediction of outcome in cardiac arrest subjects treated with hypothermia: a literature review. Journal of clinical monitoring and computing, 32(6), pp.977-992.